

## ELUCID IV: GALAXY QUENCHING AND ITS RELATION TO HALO MASS, ENVIRONMENT, AND ASSEMBLY BIAS

HUIYUAN WANG<sup>1,2</sup>, H.J. MO<sup>3,4</sup>, SIHAN CHEN<sup>1</sup>, YANG YANG<sup>1</sup>, XIAOHU YANG<sup>5,6</sup>, ENCI WANG<sup>1,2</sup>, FRANK C. VAN DEN BOSCH<sup>7</sup>, YIPENG JING<sup>5,6</sup>, XI KANG<sup>8</sup>, WEIPENG LIN<sup>9</sup>, S.H. LIM<sup>3</sup>, SHUIYAO HUANG<sup>3</sup>, YI LU<sup>11</sup>, SHIJIE LI<sup>5,6</sup>, WEIGUANG CUI<sup>10</sup>, YOUCAI ZHANG<sup>11</sup>, DYLAN TWEED<sup>5,6</sup>, CHENGLIANG WEI<sup>8</sup>, GUOLIANG LI<sup>8</sup> AND FENG SHI<sup>11</sup>

*Draft version April 18, 2022*

### ABSTRACT

We examine the quenched fraction of central and satellite galaxies as a function of galaxy stellar mass, halo mass, and the matter density of their large scale environment. Matter densities are inferred from our ELUCID simulation, a constrained simulation of local Universe sampled by SDSS, while halo masses and central/satellite classification are taken from the galaxy group catalog of Yang et al. The quenched fraction for the total population increases systematically with the three quantities. We find that the ‘environmental quenching efficiency’, which quantifies the quenched fraction as function of halo mass, is independent of stellar mass. And this independence is the origin of the stellar mass-independence of density-based quenching efficiency, found in previous studies. Considering centrals and satellites separately, we find that the two populations follow similar correlations of quenching efficiency with halo mass and stellar mass, suggesting that they have experienced similar quenching processes in their host halo. We demonstrate that satellite quenching alone cannot account for the environmental quenching efficiency of the total galaxy population and the difference between the two populations found previously mainly arises from the fact that centrals and satellites of the same stellar mass reside, on average, in halos of different mass. After removing these halo-mass and stellar-mass effects, there remains a weak, but significant, residual dependence on environmental density, which is eliminated when halo assembly bias is taken into account. Our results therefore indicate that halo mass is the prime environmental parameter that regulates the quenching of both centrals and satellites.

*Subject headings:* dark matter - large-scale structure of the universe - galaxies: halos - methods: statistical

### 1. INTRODUCTION

In the low-redshift universe, galaxies are observed to exhibit bimodal distributions in their colors and specific star formation rates. According to these bimodal distributions, galaxies can be divided into two distinctive sequences, a red sequence of galaxies quenched in star formation, and a blue sequence of star-forming galaxies (e.g. Strateva et al. 2001; Blanton et al. 2003; Baldry et al. 2004; Brinchmann et al. 2004). The bimodal distribution is correlated with galaxy mass, with the red

sequence dominated by massive galaxies, while the blue population by lower-mass ones. Furthermore, it is also known that the red, quiescent galaxies tend to reside in high density regions, while the blue star-forming galaxies display an opposite trend with environments (e.g. Oemler 1974; Dressler 1980; Hogg et al. 2003; Kauffmann et al. 2004; Baldry et al. 2006; Peng et al. 2010; Zheng et al. 2017). All these suggest that the mechanisms responsible for quenching star formation in a galaxy must be related to galaxy mass as well as to the environment.

In the current cold dark matter (CDM) cosmogony, galaxies are assumed to form and evolve within dark matter halos (e.g. White & Rees 1978; Mo, van den Bosch & White 2010). Lower-mass halos on average form earlier and subsequently merge to form more massive ones. In this process, the galaxy that forms on the main branch of a halo merging tree is expected to be the dominant galaxy residing near the center of the halo (the central galaxy), while other galaxies that form in the sub-branch progenitor halos, are expected to orbit the central as satellite galaxies. These two populations of galaxies are expected to have experienced different processes that quench their star formation: while supernovae and active galactic nuclei (AGNs) feedbacks, and shock heating of cold accretion flow may affect both central and satellite galaxies, processes like ram pressure and tidal stripping are believed to operate only on satellite galaxies (e.g. White & Frenk 1991; Kang et al. 2005; Dekel & Birnboim 2006; Bower et al. 2006; Croton et al. 2006; Kereš et al. 2009; Lu et al. 2011; Guo et al. 2011; Vogelsberger et al. 2014; Schaye et al. 2015). These models have successfully re-

<sup>1</sup>Key Laboratory for Research in Galaxies and Cosmology, Department of Astronomy, University of Science and Technology of China, Hefei, Anhui 230026, China; why-wang@mail.ustc.edu.cn

<sup>2</sup>School of Astronomy and Space Science, University of Science and Technology of China, Hefei 230026, China

<sup>3</sup>Department of Astronomy, University of Massachusetts, Amherst MA 01003-9305, USA

<sup>4</sup>Astronomy Department and Center for Astrophysics, Tsinghua University, Beijing 10084, China

<sup>5</sup>Department of Astronomy, Shanghai Jiao Tong University, Shanghai 200240, China

<sup>6</sup>IFSA Collaborative Innovation Center, Shanghai Jiao Tong University, Shanghai 200240, China

<sup>7</sup>Department of Astronomy, Yale University, P.O. Box 208101, New Haven, CT 06520-8101, USA

<sup>8</sup>Purple Mountain Observatory, the Partner Group of MPI für Astronomie, 2 West Beijing Road, Nanjing 210008, China

<sup>9</sup>School of Physics and Astronomy, Sun Yat-Sen University, Guangzhou 510275, China

<sup>10</sup>Departamento de Física Teórica, Módulo 15, Facultad de Ciencias, Universidad Autónoma de Madrid, E-28049 Madrid, Spain

<sup>11</sup>Shanghai Astronomical Observatory, Nandan Road 80, Shanghai 200030, China

produced many global properties of observed galaxies. However, there are still significant discrepancies between model predictions incorporating these processes and observational data in terms of the fraction of the quenched population (see e.g. Hirschmann et al. 2014; Vogelsberger et al. 2014; Henriques et al. 2016), indicating that our understanding of the quenching processes is still incomplete.

Observing correlations between galaxy properties and different aspects of their environment could help to distinguish different galaxy formation models. A variety of quantities have been used to describe the environment around a galaxy (Haas, Schaye & Jeason-Daniel 2012). These environmental parameters are usually designed for different purposes, and an optimal decision has to be made for a specific question (Leclercq et al. 2016). The traditional environmental parameter is the (projected) number density of galaxies, which is often adopted in observational studies of galaxy properties on various scales (e.g. Dressler 1980; Hogg et al. 2003; Kauffmann et al. 2004; Hirschmann et al. 2014). It can be directly obtained from the galaxy redshift survey without any additional assumption. The other widely used parameter is the host halo mass (e.g. Weinmann et al. 2006; Wetzel, Tinker & Conroy 2012; Woo et al. 2013), which is closely linked to galaxy formation in the CDM paradigm. Indeed, the halo occupation distribution (HOD) models (e.g. Jing et al. 1998; Peacock & Smith 2000; Zheng et al. 2005; Zu & Mandelbaum 2016), conditional luminosity function (CLF) models (e.g., Yang et al. 2003; van den Bosch et al. 2007), abundance matching models (e.g., Mo et al. 1999; Kravtsov et al. 2004; Vale & Ostriker 2006; Behroozi, Conroy, & Wechsler 2010; Hearin & Watson 2013) and halo-based empirical models (e.g., Yang et al. 2013; Lu et al. 2014, 2015; Moster, Naab & White 2017) have all used halo masses to link galaxies to dark matter halos.

Using halo mass inferred from galaxy group catalog (Yang et al. 2007) as environmental parameter, Weinmann et al. (2006) found that the quenched fraction of satellite galaxies is much lower than that in model predictions and increases strongly with host halo mass (see also Liu et al. 2010; Wetzel et al. 2012). This has motivated later semi-analytic galaxy formation models (SAMs) to employ an incremental stripping of hot gas associated with satellites through ram-pressure and tidal stripping (e.g. Kang & van den Bosch 2008; Font et al. 2008; Weinmann et al. 2010; Guo et al. 2011; Henriques et al. 2015). Moreover, halo mass is also found to have significant impact on the quenching of star formation in centrals of given galaxy masses (Weinmann et al. 2006; Woo et al. 2013; 2015; Bluck et al. 2014; 2016). Here, AGN feedback is thought to be the major quenching mechanism, and its strength is likely to depend on halo mass (e.g. Croton et al. 2006; Henriques et al. 2016), qualitatively consistent with the observation results.

In addition to environmental effects that are confined within halos, there are also observational indications that the environmental effects may operate on scales beyond their boundaries. For example, at a fixed halo mass, the clustering of galaxy groups is found to depend on the star formation rate and color of the central galaxies (Yang, Mo, & van den Bosch 2006; Lacerna, Padilla,

& Stasyszyn 2014). Similarly, Kauffmann et al. (2013) found that the star formation rates of central galaxies are correlated with that of their neighbours on scales up to several Mpc, far beyond their halo virial radii (see also Berti et al. 2017, and references therein). These results suggest that large scale environments may also affect the star formation of galaxies embedded in them. However, it is unclear whether this is due to a causal connection between star formation and large-scale environments, or is produced by a correlation induced by some intermediate connections. For example, such large-scale effects may be produced by the dependence of star formation on halo assembly history (see e.g. Hearin, Watson, & van den Bosch 2015; Lim et al. 2016; Tinker et al. 2016; Zentner et al. 2016), combined with halo assembly bias that links halo formation with large-scale structure (e.g. Gao, Springel, & White 2005; Wechsler et al. 2006; Jing, Suto & Mo 2007), or may be produced by the preheating of the intergalactic gas owing to the formation of large scale structure (e.g. Mo et al. 2005; Kauffmann et al. 2013).

Using galaxy number density as environmental parameter, Baldry et al. (2006) found that the quenched fraction depends both on galaxy stellar mass and environmental density, and the dependence can be well described by a simple functional form. Peng et al. (2010) studied the environmental quenching efficiency, which is defined as the probability for a galaxy to be quenched in high-density regions relative to that in low-density regions, where environmental effects are expected to be weak. Remarkably, the efficiency defined in this way is found to be almost independent of stellar mass. Subsequently, Peng et al. (2012) suggested that the independence may be explained if environmental quenching is assumed to be important only for satellite galaxies, and if both the quenching efficiency of satellite galaxies and the satellite fraction are independent of galaxy mass. However, these assumptions are not supported by the results obtained for centrals from galaxy groups, which clearly show that environmental quenching of central galaxies is also important (e.g. Weinmann et al. 2006; Woo et al. 2013; 2015), and by the results for satellites, which show that both the quenching efficiency (Knobel et al. 2015) and satellite fraction (Mandelbaum et al. 2006; Cooray 2006; Tinker et al. 2007; van den Bosch et al. 2007) depend on galaxy mass.

The difference between centrals and satellites also attracted particular attention (e.g. van den Bosch et al. 2008; Skibba 2009; Wetzel et al. 2012; 2013; Peng et al. 2012; Hirschmann et al. 2014; Knobel et al. 2015; Spindler & Wake 2017). It has been found that the quenched fraction of the central population is lower than that of satellites of the same mass. This difference has been used to quantify the efficiency of various satellite-specific quenching processes, such as strangulation, tidal stripping and ram-pressure stripping (van den Bosch et al. 2008). However, Knobel et al. (2015) found that centrals and satellites of the same mass respond to their environments in a similar way, as long as centrals have massive satellites. Moreover, Hirschmann et al. (2014) studied the failures of current galaxy formation models in matching observational data and suggested that centrals and satellites should be treated not as differently in their response to environments as previously assumed.

Clearly, more investigations are required in order to understand these contradictory results in the literature. It is essential to identify and characterize the contribution to the quenching of star formation of the relevant parameters, such as galaxy stellar mass, halo properties and large-scale density field. In particular, it is important to see whether the independence of environmental quenching efficiency on galaxy mass can be reproduced if only halo masses and halo assembly bias are taken into account, and what roles centrals and satellites play in establishing the galaxy-mass independence of the quenching efficiency found earlier, and whether the star formation quenching in centrals and satellites is dominated by different processes.

In this paper, the fourth of a series, we use the environmental information provided by the ELUCID project and galaxy groups selected from the Sloan Digital Sky Survey (SDSS; York et al. 2000) to investigate the quenching of galaxies in different environments. The ELUCID project (Wang et al. 2014; 2016; Tweed et al. 2017) aims to reconstruct the initial conditions responsible for the formation of the structures in the observed low-redshift universe, and to recover the mass distribution in the local universe by constrained simulations. The constrained simulations give the full information about the dynamical state and formation history of the large scale structure within which the observed galaxies reside. This provides an unique opportunity to systematically investigate the quenched population of galaxies of different masses in different environments.

Our paper is organized as follows. In Section 2, we describe the galaxy sample, group catalog and environmental quantities used for our analysis. Section 3 shows how the quenched galaxy population depends on galaxy mass, halo mass and environmental density for the total population, as well as separately for the central and satellite populations. In Section 4, we investigate the galaxy stellar mass independence of the environmental quenching efficiency using the matter density field as inferred from our ELUCID simulation, with a special focus on the role of central and satellite galaxies. In Section 5, we investigate the quenching efficiencies using halo mass as environmental parameter. In Section 6 we discuss the implications of our results by comparing the data to three simple models that incorporate the dependence on galaxy stellar mass, halo mass, environmental density, and halo assembly history. In Section 7 we discuss whether central galaxies are special in their quenching properties in comparison with satellites. Finally, we summarize our results and discuss their implications in Section 8.

## 2. GALAXY SAMPLE AND ENVIRONMENTAL QUANTITIES

### 2.1. The galaxy sample

The galaxy sample used here is extracted from the New York University Value-added Galaxy Catalog (NYU-VAGC, Blanton et al. 2005) of the SDSS DR7 (Abazajian et al. 2009). We select all galaxies in the main galaxy sample, with  $r$ -band apparent magnitudes  $\leq 17.72$ , and with redshift completeness  $C \geq 0.7$ , and within the reconstruction region of ELUCID simulation (see below and Wang et al. 2016 for the details). The first two selection criteria ensure that most of the selected galaxies are

contained in the Yang et al. (2007) group catalog (with extension to DR7), and the third ensures that we have reliable estimates of our galaxies' environmental densities. Among these galaxies, 1,707 are members of groups that have only a fraction of  $0 < f_{\text{edge}} \leq 0.6$  of their virial volumes contained within the survey boundary. These galaxies are removed from our sample (see Yang et al. 2007). A total of 4,233 galaxies that do not have star formation rate estimates are also discarded. Our final sample contains 317,791 galaxies.

Stellar masses for these galaxies, indicated by  $m$  (with unit  $h^{-2}M_{\odot}$ ), are computed using the relations between stellar mass-to-light ratio and  $(g-r)$  color as given in Bell et al. (2003), adopting a Kroupa (2001) initial mass function (IMF). We refer to Yang et al. (2007) for details. Star formation rates (SFR) for these galaxies are taken from the the MPA-JHU DR7 release website<sup>12</sup>, which are estimated by using an updated version of the method presented in Brinchmann et al. (2004) and calibrated to the Kroupa IMF. For given galaxy stellar mass, the distribution of SFR is known to be bimodal (e.g. Brinchmann et al. 2004), with a high SFR mode corresponding to the star forming population and a low SFR mode corresponding to a quenched population. In this paper, we adopt the division line proposed by Woo et al. (2013) to separate the two populations:

$$\log \text{SFR} = 0.64 \log m - 1.28 \log h - 7.22, \quad (1)$$

where the reduced Hubble constant  $h$  (Hubble constant in units of  $100 \text{ km s}^{-1} \text{ Mpc}^{-1}$ ) is used to transfer the unit of the stellar mass from  $h^{-2}M_{\odot}$  used here to  $M_{\odot}$  used in Woo et al. (2013).

In our analyses, each galaxy is assigned a weight  $w = 1/(V_{\text{max}}C)$  to take into account the Malmquist bias and redshift (spectroscopic) incompleteness, with the latter taken from the NYU-VAGC. Since the geometry of our reconstruction region is not regular, we calculate  $V_{\text{max}}$  in the following way. For each galaxy, we first obtain its Petrosian photometry in  $ugriz$  bands and its redshift. We then use these data as input to the  $K$ -correction utilities (v4.2) of Blanton & Roweis (2007) to estimate  $z_{\text{min}}$  and  $z_{\text{max}}$ , the minimum and maximum redshifts, between which the galaxy can be observed with the  $r$ -band limit of 17.72 mag. Finally, we measure  $V_{\text{max}}$  as the volume of the reconstruction region that is between  $z_{\text{min}}$  and  $z_{\text{max}}$ .

### 2.2. Host halos of galaxies

Galaxy groups and clusters (hereafter referred to together as galaxy groups), when properly selected from a galaxy sample, can be used to represent the host dark halos of galaxies. In this paper we make use of the galaxy groups identified by Yang et al. (2012) from the SDSS DR7 to represent halos in which galaxies reside. This group catalog was constructed with the halo-based group finder developed by Yang et al. (2005), which assigns new galaxies into groups based on the size (virial radius) and velocity dispersion of the host dark halo represented by the current members assigned to a tentative group. Iterations are performed until the identification of member galaxies as well as the estimation of halo mass converge. The halo masses in the catalog are estimated

<sup>12</sup> <http://www.mpa-garching.mpg.de/SDSS/DR7/>

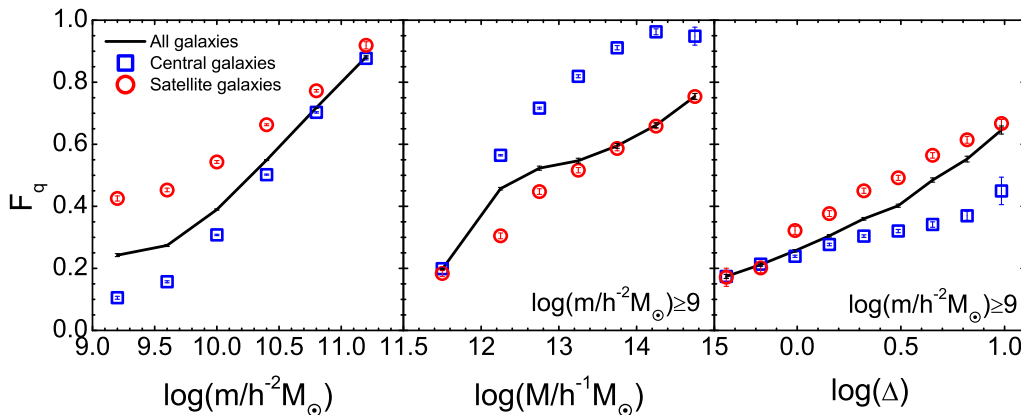


FIG. 1.— Quenched fraction of galaxies as a function of galaxy stellar mass (left panel), halo mass (middle panel), and environmental density (right panel), obtained from samples of the total (lines), central (squares) and satellite (circles) populations. The middle and right panels show the results only for galaxies with  $\log(m/h^{-2}M_{\odot}) \geq 9.0$ .

via the ranking of two mass proxies: the total luminosity or total stellar mass of all members brighter than  $M_r = -19.5 + 5 \log(h)$  in the  $r$ -band. For our analysis, we adopt the halo masses,  $M$  (with unit  $h^{-1}M_{\odot}$ ), estimated using the total stellar mass. Following common practice, we define the central galaxy of a group to be the most massive member, and all other members are referred to as satellites. The reconstruction region is restricted to the redshift range  $0.01 < z < 0.12$ , where groups with  $\log(M) \gtrsim 12$  are complete.

### 2.3. Environmental density

In Wang et al. (2016; hereafter paper III), we presented a series of methods to reconstruct the initial density field that is responsible for the galaxy distribution in the local Universe, and we used a high-resolution N-body simulation to evolve the initial conditions to the present-day. These simulation results can be used to obtain reliable estimates for the environmental densities within which the observed SDSS galaxies reside.

The reconstruction is restricted to the Northern Galactic Cap of the SDSS DR7 region and to the redshift range  $0.01 \leq z \leq 0.12$ . In order to avoid problems near the survey boundary, where the reconstruction is less reliable, we exclude galaxies and groups whose distances to the SDSS survey boundary are smaller than  $5 h^{-1} \text{Mpc}$ . For each galaxy, we correct for its redshift-space distortions (see Paper III, Wang et al. 2012 and Shi et al. 2016, for details) and estimate its real-space location. The environmental density for a galaxy is determined by computing the matter density, smoothed with a Gaussian kernel of  $4 h^{-1} \text{Mpc}$ , at its real-space location in our constrained simulation. Tests based on mock galaxy catalogs demonstrate that the uncertainties in this density estimate are typically 0.10 dex. In what follows, we quantify the matter density for each galaxy using the quantity

$$\Delta = \rho / \bar{\rho}, \quad (2)$$

where  $\rho$  is the smoothed mass density at the location of the galaxy, and  $\bar{\rho}$  is the mean density of the universe.

In the literature, one environmental indicator commonly used is the local number density (or over-density) of galaxies. Our tests show that the galaxy densities are positively correlated with the mass densities, although the scatter is rather large (see also Baldry et al. 2006). Because of the redshift distortion effect and the complicated correlation with underlying mass density, galaxy density hampers a meaningful interpretation of its correlation between galaxy properties (see Weinberg et al. 2006 and Woo et al. 2013). Therefore, we consider the matter densities,  $\Delta$ , used here to be a superior, and more physical, quantity to characterize the large-scale environment of a galaxy.

## 3. THE QUENCHED POPULATIONS

In this section we examine how quenching of star formation depends on the intrinsic and environmental properties of galaxies. For any subset of galaxies with a given set of properties  $\{g\}$ , we calculate the average quenched fraction as

$$F_q(\{g\}) = \frac{\sum_{i \in \{g\}} q_i w_i}{\sum_{i \in \{g\}} w_i}, \quad (3)$$

where  $w_i$  is the weight for a galaxy  $i$ , and  $q_i$  is set to 1 for a quenched galaxy, otherwise zero. In our following analysis, we will consider the total population, and the central and satellite populations separately. The quenched fractions of the sub-populations are denoted by  $F_{q,c}$  (centrals) and  $F_{q,s}$  (satellites), respectively.

### 3.1. Marginalized dependence on stellar mass, halo mass and density

Figure 1 shows, for the whole population and for centrals and satellites separately, the quenched fraction of galaxies as a function of galaxy stellar mass, halo mass and environmental mass density. The quenched fractions as a function of one of the three parameters are obtained by marginalizing over the other two parameters. Note that we only consider galaxies with  $\log(m) \geq 9.0$  and results are shown only for these galaxies in the left two panels. In this and the following figures, error bars are

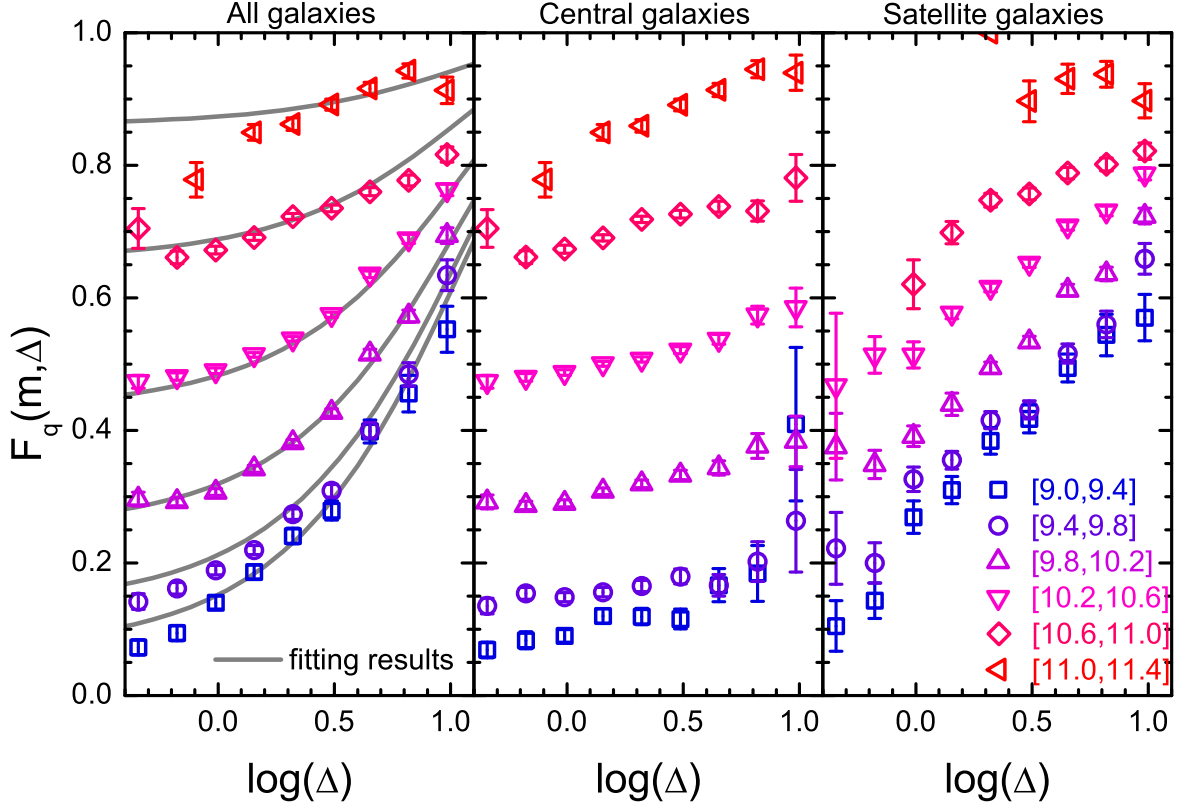


FIG. 2.— Quenched fractions of galaxies in given stellar mass bins as functions of the environmental density, obtained from samples of the total (left panel), central (middle panel) and satellite (right panel) populations. The curves in the left panel are model fits to the data (see text).

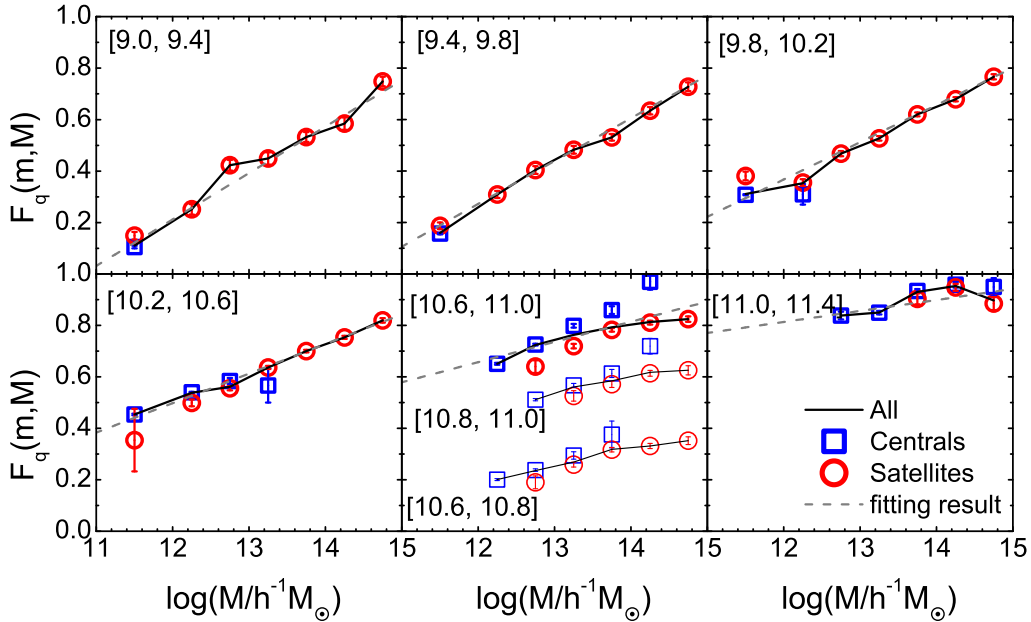


FIG. 3.— Quenched fraction as a function of halo mass. Galaxies are divided into six mass bins as shown in the panels. The squares and circles show the results for centrals and satellites, respectively. The solid lines show the results for all galaxies in the corresponding mass bins. The gray dashed lines show the fitting of the total population with Equation (14). For galaxies with  $10.6 \leq \log(m) \leq 11$ , we split them into two sub-samples with narrower mass ranges as indicated in the panel. For clarity, the two sub-samples are shifted down by 0.25 for high mass bin and 0.45 for low mass bin, respectively.

all evaluated from 1,000 bootstrap re-samplings and only data points that contain at least 10 galaxies are shown.

It is clear that the quenched fraction increases with increasing stellar mass, halo mass and environmental density, consistent with previous studies (e.g. Brinchmann et al. 2004; Weinmann et al. 2006; Baldry et al. 2006). These correlations are often considered as observational evidence for quenching processes, such as mass quenching, halo quenching and environmental quenching. We then examine centrals and satellites separately. At given stellar mass or density, satellites tend to be more often quenched than centrals. However, the trend is reversed if halo mass is used instead as the control parameter. It is well known that more massive galaxies tend to live in more massive halos and more massive halos tend to reside in higher density regions, and so it is not obvious whether the density dependence reflects a causal connection or is induced by the correlation between halo mass and density. In order to disentangle the different effects, we need to examine the joint distribution of the quenched population with respect to the parameters in question (see below).

### 3.2. Dependence on stellar mass and environmental density

We first disentangle the dependencies of the quenched fraction on stellar mass and environmental density. The left panel of Figure 2 shows the quenched fraction of the total population,  $F_q(m, \Delta)$ , as a function of the environmental density for galaxies in various stellar mass bins. Consistent with the marginalized result, there is significant dependence on  $\Delta$ , even for galaxies in a given narrow  $m$  bin. The dependence is seen to be stronger at low  $m$  and weaker at the lower  $\Delta$  end. At a given  $\Delta$ , the quenched fraction increases with  $m$ , and the increase is more significant for galaxies of lower masses.

We then investigate the quenched fractions separately for the central and satellite populations and present the results in the middle and right panels of Figure 2. For central galaxies, the  $\Delta$ -dependence is rather weak for all stellar mass bins in comparison to the result shown in the right panel of Figure 1. This suggests that the marginalized  $\Delta$ -dependence for centrals is primarily due to the fact that more massive centrals tend to reside in higher density region. In contrast, for satellites, the  $\Delta$ -dependence is strong in most of the stellar mass bins. In particular, the marginalized  $\Delta$ -dependence is very similar to that for the lowest stellar mass galaxies, indicating that the marginalized result for satellites is dominated by low-mass galaxies over the whole density range. At given  $\Delta$ , the  $m$ -dependence is significant for both centrals and satellites. The  $m$ -dependence for centrals is similar to that for satellites at low  $\Delta$ , but is stronger at high  $\Delta$ , suggesting that the difference shown in the marginalized  $m$ -dependence between the two populations is mainly caused by the difference in the high density region. These results are in qualitative agreement with the results previously obtained by Peng et al. (2010; 2012) and Knobel et al. (2015).

### 3.3. Dependence on stellar mass and halo mass

Figure 3 shows the quenched fraction as a function of halo mass for galaxies in different stellar mass bins. At

a given  $m$ , the quenched fraction increases with  $M$ , and the increase is steeper for lower mass galaxies. These trends are consistent with those obtained before (e.g. Weinmann et al. 2006; Wetzel et al. 2012). Most intriguingly, the behaviors of central and satellite galaxies are almost indistinguishable, although it is important to stress that the halo mass range covered by central galaxies is rather limited, in particular for galaxies with low masses. This suggests that the difference between centrals and satellites found in the marginalized dependencies on  $m$  and  $M$  are mainly caused by the different  $m$  and  $M$  ranges covered by the two populations. For example, satellites usually reside in more massive halos than centrals of the same stellar mass, this combined with the  $M$ -dependence of the quenched fraction can explain why the quenched fraction for satellites is higher than that for centrals of the same stellar mass (left panel of Figure 1). Similarly, since by construction centrals are more massive than satellites in halos of a given mass, centrals are expected to be more often quenched than satellites because of the  $m$ -dependence (middle panel of Figure 1).

For the stellar mass bin  $10.6 \leq \log(m) \leq 11$ , the quenched fraction of centrals appears to be somewhat higher than for satellites in the same halo mass bin. However, upon closer inspection, we find that this is mainly an artifact of the finite bin-sizes used, combined with the fact that at given halo mass, the satellite galaxies are strongly biased towards  $\log(m) \sim 10.6$ , while centrals are biased towards  $\log(m) \sim 11$ . To demonstrate this, we split the galaxies in this mass bin into two sub-samples at  $\log(m) = 10.8$ . The results for these two sub-samples are shown in the bottom left panel of Figure 3. As one can see, this significantly reduces the differences between the centrals and satellites, and we therefore conclude that there is no significant difference in the halo mass dependence of the quenched fraction between centrals and satellites.

We note again that numerous previous studies (e.g., van den Bosch et al. 2008; Weinmann et al. 2009; Pasquali et al. 2010; Wetzel et al. 2012; Peng et al. 2012; Knobel et al. 2013; Bluck et al. 2014; Fossati et al. 2017) have shown that, at a given stellar mass, satellites are more often quenched than centrals and suggested that some satellite-specific environmental processes have played important roles in quenching satellite galaxies. However, our results portray a different picture; centrals and satellites follow the same correlation between quenched fraction and host halo mass, suggesting that they experienced similar environment-dependent quenching, and the only reason that satellite and centrals appear different at fixed stellar mass is that they sample different ranges in host halo mass. Further investigations on this are presented in Sections 6 and 7.

### 3.4. Dependence on halo mass and environmental density

It is known that more massive halos tend to locate in higher density regions, an effect usually referred to as halo bias (e.g. Mo & White 1996). Therefore the density dependence shown in Figure 2 and the halo mass dependence shown in Figure 3 may be connected. To examine this, we split galaxies further into four sub-samples based on  $\Delta$  and calculate the quenched fraction as a function of  $M$ . The results are shown in Figure 4. Overall, the

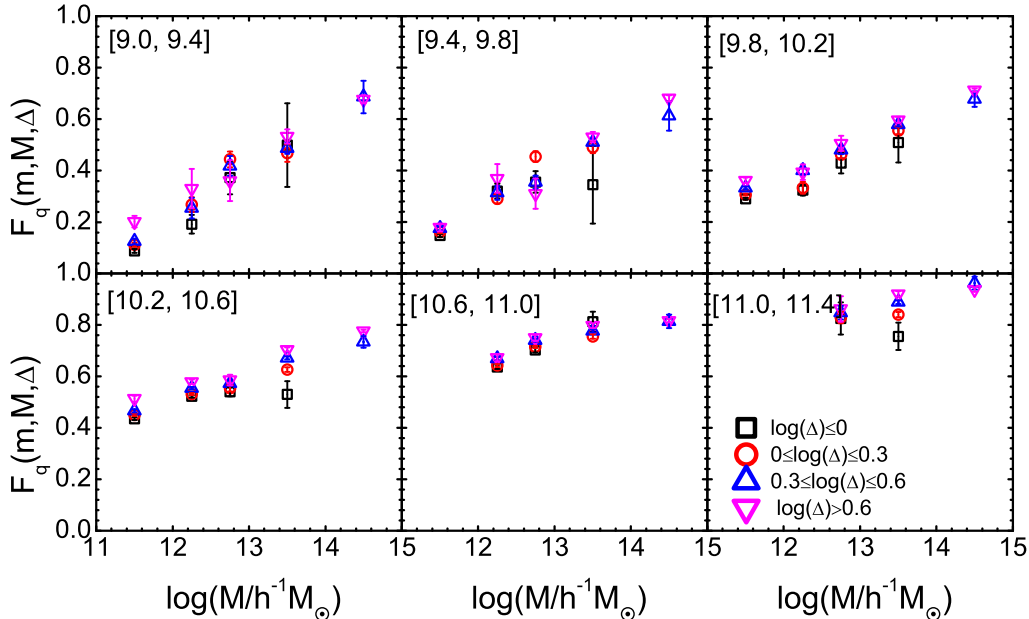


FIG. 4.— Quenched fraction as a function of halo mass for galaxies with different  $\Delta$  and  $m$  as indicated in the panels.

$M$ -dependence of the quenched fraction is similar for different sub-samples of  $\Delta$ , suggesting that halo mass may be the dominating factor in determining the quenched fraction.

However, for a given  $M$ , there is a weak but systematic trend of increasing quenched fraction with increasing  $\Delta$ . This suggests that factors other than halo mass affect galaxy quenching, and is broadly consistent with some previous findings that galaxy groups of a given halo mass have different clustering properties depending on the color or star formation of their member galaxies (e.g. Yang et al. 2006). All of this is most likely related to assembly bias (Gao et al. 2005), the fact that halo bias depends not only on halo mass, but also on other halo properties such as assembly history, if the quenching processes depend on these additional halo properties. Unfortunately, the observational sample is still too small, and the uncertainties in the density dependence shown in Figure 4 are still too large, to draw any quantitative conclusions. We will revisit this issue in Section 6.

#### 4. DENSITY-BASED ENVIRONMENTAL QUENCHING EFFICIENCIES

A useful parameter to quantify the efficiency of galaxy quenching is the relative environmental quenching efficiency (hereafter ‘quenching efficiency’ for brevity)

$$\varepsilon(m, \Delta|\Delta_0) \equiv \frac{F_q(m, \Delta) - F_q(m, \Delta_0)}{1 - F_q(m, \Delta_0)}. \quad (4)$$

(Peng et al. 2010), which specifies the probability for a star-forming galaxy of mass  $m$  to be quenched when it transits from an environment characterized by some zero-point matter density,  $\Delta_0$ , to a region with  $\Delta$ . We choose  $\Delta_0$  to correspond to the lowest-density environment probed by our data, as the environmental effects are expected to be minimal in these void-like environments. As shown in Figure 2, the quenched fraction of

galaxies, in most of the stellar mass bins, has the lowest value at  $\log \Delta \leq 0$ , where the  $\Delta$ -dependence of the quenched fraction is also weak. We thus choose galaxies with  $\log \Delta \leq 0$  to define the zero point.

##### 4.1. A dearth of stellar mass dependence for the total population

The upper-left panel of Figure 5 shows the quenching efficiency  $\varepsilon(m, \Delta|\Delta_0)$  of the total population as a function of  $\Delta$ . As one can see, the efficiency is close to zero at  $\Delta \sim \Delta_0$ , by definition, and increases rapidly with  $\Delta$ . Remarkably, the efficiency is almost independent of  $m$  over the range  $9 \leq \log(m) \leq 11$ . To see this more clearly, we show  $\varepsilon(m, \Delta|\Delta_0)$  as a function of  $m$  for various  $\Delta$  bins in Figure 6 as black squares. The quenching efficiency is almost a constant in the entire mass range, except for the highest stellar mass bin. This is in good agreement with Peng et al. (2010), although they used galaxy number density instead of the more physical matter density used here. The efficiency for the highest stellar mass bin is higher than for the other stellar mass bins, but the uncertainties are large. Note that there are only very few massive galaxies in low density regions with  $\Delta < 1$ , which can produce a large statistical uncertainty in the denominator of Eq. (4). The discrepancy for the highest  $m$  bin is, therefore, not conclusive. We will come back to this issue in Section 6.

Baldry et al. (2006) found that the quenched fraction can be fitted by a very simple equation:

$$F_q(m, \Delta) = 1 - \exp \left[ - \left( \frac{\Delta}{\Delta_*} \right)^b \right] \exp \left[ - \left( \frac{m}{m_*} \right)^d \right]. \quad (5)$$

Inserting it into Equation (4), we obtain

$$\varepsilon(m, \Delta|\Delta_0) = 1 - \exp \left[ - \left( \frac{\Delta}{\Delta_*} \right)^b + \left( \frac{\Delta_0}{\Delta_*} \right)^b \right]. \quad (6)$$

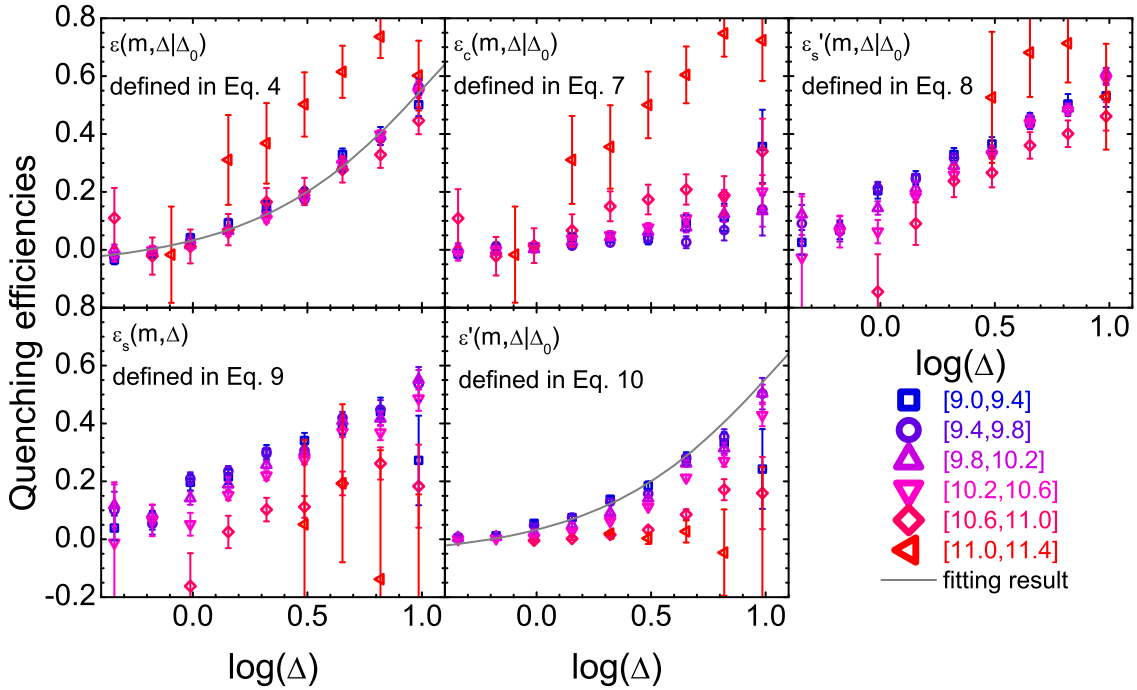


FIG. 5.— Quenching efficiencies defined by the equations shown in each panel as a function of environmental density  $\Delta$  for galaxies of different masses as indicated in the bottom right panel. The gray line shown in the top left and bottom middle panels is the fitting curve [fitting formula Equation (6)] of the data shown in the top left panel. See the text for the details. Note that, for the most massive galaxies, two data points at  $\log \Delta \sim 0.3$  and  $1.0$  lie outside of the figure boundary in the bottom left panel, and one data point at  $\log \Delta \sim 1.0$  lies outside the boundary in the bottom middle panel.

We use this equation to fit the  $\varepsilon$  data points, with  $\log \Delta_0 = -0.2$ , which is the median value for galaxies with  $\log \Delta_0 \leq 0$ . The best fit gives  $\Delta_* = 11.5 \pm 0.26$  and  $b = 0.975 \pm 0.035$  (see Figure 5 for the fitting curve). We then use Equation (5) to fit the quenched fraction for the total population with  $\Delta_* = 11.5$  and  $b = 0.975$ . The best fit values for the other two parameters are  $m_* = 5.29 \pm 0.04 \times 10^{10} h^{-2} M_\odot$  and  $d = 0.749 \pm 0.006$ , and the results are shown in the left panel of Figure 2. These fitting results are presented here as a convenient way to represent the data.

#### 4.2. Central versus satellite populations

For central galaxies, we define a quenching efficiency similar to Equation (4):

$$\varepsilon_c(m, \Delta | \Delta_0) = \frac{F_{q,c}(m, \Delta) - F_{q,c}(m, \Delta_0)}{1 - F_{q,c}(m, \Delta_0)}, \quad (7)$$

where  $F_{q,c}(m, \Delta)$  is the quenched fraction of central galaxies. Here again we use galaxies at  $\log \Delta_0 \leq 0$  to calculate  $F_{q,c}(m, \Delta_0)$ . So defined, this efficiency characterizes the probability for a star forming central to quench if it were to move to a higher density environment,  $\Delta$ , while remaining a central. As is evident from the upper-middle panel of Figure 5,  $\varepsilon_c$  has a much weaker dependence on  $\Delta$  than the corresponding quenching efficiency of the total population. Nevertheless, even for centrals there is a significant tendency for  $\varepsilon_c$  to increase with  $\Delta$ . Moreover, there is also a trend for  $\varepsilon_c$  to increase with stellar mass (see also Figure 6), in particular at high  $\Delta$ . As for the total population, the most massive

bin has very few galaxies with  $\log \Delta \leq 0$ , so that the corresponding  $\varepsilon_c$  carries large uncertainties.

Similarly, we can define a quenching efficiency for satellite galaxies. Unfortunately, the total number of satellites at  $\log \Delta \leq 0$  is small, and so the derived efficiency will have large uncertainties. However,  $F_{q,s}(m, \Delta_0)$  is close to  $F_{q,c}(m, \Delta_0)$  for most of stellar mass bins where both can be measured reliably (Figure 2). We thus define an alternative efficiency for satellites as

$$\varepsilon'_s(m, \Delta | \Delta_0) = \frac{F_{q,s}(m, \Delta) - F_{q,c}(m, \Delta_0)}{1 - F_{q,c}(m, \Delta_0)}. \quad (8)$$

The results are shown in the upper-right panel of Figure 5. As one can see,  $\varepsilon'_s(m, \Delta | \Delta_0)$  increases rapidly with  $\Delta$ , but its dependence on  $m$  is weak.

Finally we consider a satellite-specific quenching efficiency, which is defined as

$$\varepsilon_s(m, \Delta) = \frac{F_{q,s}(m, \Delta) - F_{q,c}(m, \Delta)}{1 - F_{q,c}(m, \Delta)}, \quad (9)$$

(see van den Bosch et al. 2008). Here, the central galaxies are used as the control sample (zero point) in  $(m, \Delta)$  space, against which the quenching of satellites is measured. The lower-left panel of Figure 5 shows  $\varepsilon_s$  as a function of  $\Delta$  for satellite galaxies of different masses. As one can see, the quenching efficiency increases quite rapidly with  $\Delta$  in most stellar mass bins. For a given  $\Delta$ ,  $\varepsilon_s$  decreases with  $m$ , and the decrease is larger for more massive galaxies.

As pointed out by Wetzel et al. (2013),  $\varepsilon_s$  defined

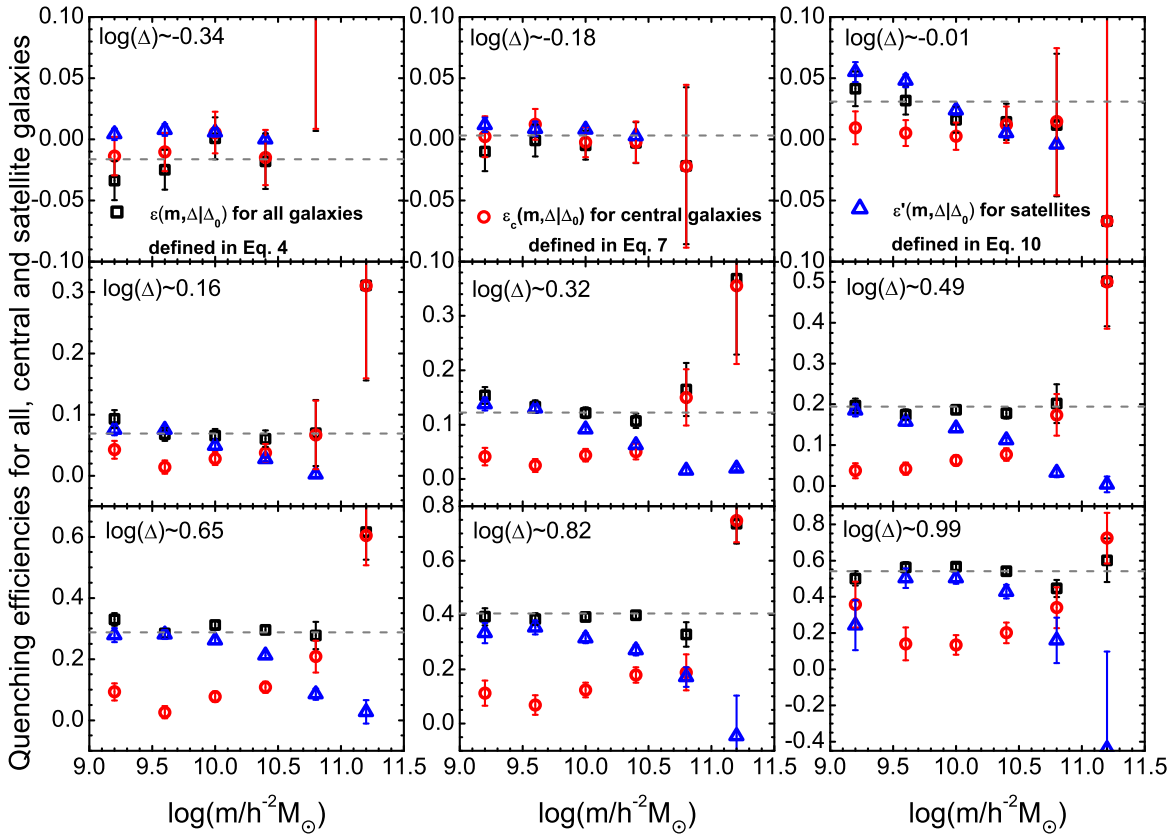


FIG. 6.— The quenching efficiencies defined by Equation (4), (7) and (10) as a function of stellar mass for various environmental densities as shown in each panel. The horizontal dashed lines show the best fitting results of Equation (6). In the top-middle panel, two data points ( $\varepsilon$  and  $\varepsilon_c$ ) at  $\log m = 11.2$  lies outside the figure boundary.

in this way actually measures a combined effect of the satellite-specific quenching processes and the evolution of central galaxies. So it is not straightforward to use it to interpret the satellite quenching efficiency. However, it does not change our conclusion in the subsequent subsection that there exists an unexpected connection between centrals and satellites.

#### 4.3. A conspiracy between centrals and satellites?

Peng et al. (2010) argued that the stellar mass independence of  $\varepsilon(m, \Delta|\Delta_0)$  can be fully understood in terms of the quenching of satellite galaxies. Assuming that the environmental effect on centrals is negligible, they wrote the environmental quenching efficiency as,

$$\varepsilon'(m, \Delta|\Delta_0) = f_s(m, \Delta)\varepsilon_s(m, \Delta), \quad (10)$$

where,  $f_s(m, \Delta)$  is the satellite fraction, and  $\varepsilon_s(m, \Delta)$  is the satellite-specific quenching efficiency of Equation. (9). Figure 7 shows the satellite fraction as a function of  $\Delta$  for galaxies in different  $m$  bins. In order to explain the  $m$ -independence of the quenching efficiency, Peng et al. (2010; 2012) suggested that both  $f_s(m, \Delta)$  and  $\varepsilon_s(m, \Delta)$  are independent of  $m$ . This is clearly inconsistent with our data shown in the lower-left panel of Figure 5 and Figure 7.

Since the hypothesis made by Peng et al. has far-reaching implications (i.e., the the environment dependence of the quenching efficiency is entirely due to the

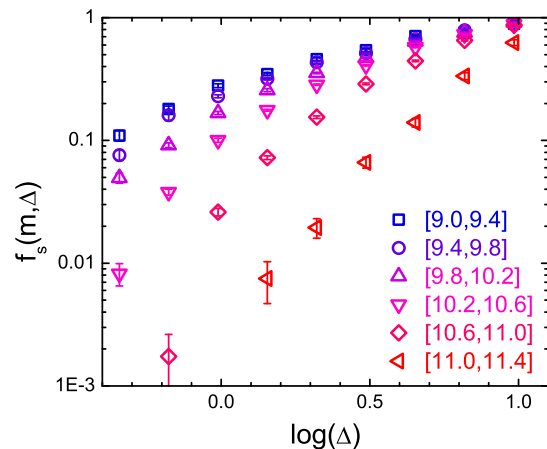


FIG. 7.— The satellite fraction as a function of  $\Delta$  at various galaxy masses. Note that the two data points at low  $\Delta$  for the two most massive galaxy bins are zero, and thus not shown in the figure.

quenching of satellites), it is important to address this discrepancy in some detail. In fact, there are a number of factors that play a role. First of all, Peng et al. used the over-density of galaxies as their environment indicator, rather than the more physical matter density used here. In addition, they used colors to split their population into

star-forming and quenched, whereas we use actual star formation rates. Since dust extinction can make a star forming galaxy appear red, and thus ‘quenched’ based on color, using actual star formation rates yields more accurate estimates of the true quenched fraction. Secondly, Peng et al., assumed  $F_{q,c}(m, \Delta)$  to be independent of  $\Delta$ , even though this is not supported by their own data. Since centrals on average reside in lower  $\Delta$  environments than satellites of the same stellar mass (e.g. Knobel et al. 2015), the average of  $F_{q,c}$  over  $\Delta$  is biased towards low-density regions. As a consequence, adopting the average of  $F_{q,c}$  can lead to an overestimation of  $\varepsilon_s$ , in particular at the high- $\Delta$  end. For low-mass galaxies, this bias is negligible, because  $F_{q,c}$  is on average much smaller than both  $F_{q,s}$  and unity. This is consistent with the weak  $m$ -dependence of  $\varepsilon_s$  we find for these galaxies. For massive galaxies, on the other hand, the value of  $F_{q,c}$  is higher and the denominator in Equation (9) smaller. This results in a significant bias that weakens the  $m$ -dependence of  $\varepsilon_s$  at the high mass end. Indeed, when taking into account the dependence of  $F_{q,c}$  on galaxy number density, Knobel et al. (2015) also found that  $\varepsilon_s$  decreases with  $m$  at a given galaxy number density (see their figure 3). Finally, as is evident from Figure 7, the satellite fraction depends strongly on  $m$ . In fact, it is well known that the satellite fraction increases with decreasing stellar mass, which has been demonstrated using galaxy group catalogs (e.g., van den Bosch et al. 2008), subhalo abundance matching (e.g., Wetzell et al. 2013), galaxy-galaxy lensing (e.g., Mandelbaum et al. 2006), galaxy clustering (e.g., Cooray 2006; Tinker et al. 2007; van den Bosch et al. 2007) and combinations thereof (e.g., Cacciato et al. 2013).

In the lower-middle panel of Figure 5, we show  $\varepsilon'$  as a function of  $\Delta$ . For low-mass galaxies with  $\log(m) \leq 10.2$ ,  $\varepsilon'$  is almost independent of  $m$ , in agreement with the hypothesis of Peng et al. (2010; 2012). However, for more massive galaxies,  $\varepsilon'$  clearly depends on  $m$ . Thus, the  $m$ -independence of  $\varepsilon$  of the total population shown in Section 4.1 is not due to the  $m$ -independence of  $f_s$  and  $\varepsilon_s$ , and the quenching efficiency of the total galaxy population cannot be explained by the quenching of satellites alone.

As shown in Figure 2, central galaxies do exhibit some weak but non-trivial  $\Delta$ -dependence in all the mass bins considered, and at  $\log(m) \geq 10.6$  the dependence is actually comparable to or slightly stronger than that for satellites. For centrals, the  $\Delta$ -dependence is stronger for more massive galaxies, a trend opposite to that seen for satellites. To understand the importance of quenching for centrals in the total population, we express the quenching efficiency for the total population in terms of  $\varepsilon_c$  and  $\varepsilon'$ . At very low density,  $\log \Delta \leq 0$ , environmental quenching is very weak and  $f_s(m, \Delta)$  is quite small. Thus, to good approximation  $F_q(m, \Delta_0) \approx F_{q,c}(m, \Delta_0)$ , and we can rewrite Equation (4) as

$$\begin{aligned} \varepsilon(m, \Delta | \Delta_0) &\simeq \frac{F_q(m, \Delta) - F_{q,c}(m, \Delta_0)}{1 - F_{q,c}(m, \Delta_0)} \\ &= \varepsilon_c(m, \Delta | \Delta_0) + [1 - \varepsilon_c(m, \Delta | \Delta_0)] \varepsilon'(m, \Delta | \Delta_0), \end{aligned} \quad (11)$$

where the second equation is obtained by inserting Equations (7) and (9) into the right-hand-side of the first line. Note that this reduces to Equation (10) in the limit

$\varepsilon_c \rightarrow 0$ . Using Equation (11) to compute the quenching efficiencies yields the results that are in excellent agreement with those shown in Figure 5 obtained using the original definition [Equation. (4)]. Since the difference in all  $m$  bins is less than 0.03, we do not show the results. The good agreement justifies our approximation that  $F_q(m, \Delta_0) \approx F_{q,c}(m, \Delta_0)$ .

Note once more that  $\varepsilon(m, \Delta | \Delta_0)$  reveals only a very weak dependence on  $m$ , except for the most massive galaxies, for which the statistics is extremely poor (see Section 4.1). It seems to conflict with the fact that  $\varepsilon$  is the combination of  $\varepsilon_c$  and  $\varepsilon'$ , which both strongly depend on  $m$ . To understand this apparent discrepancy, we show  $\varepsilon$ ,  $\varepsilon_c$  and  $\varepsilon'$  as a function of  $m$  for various  $\Delta$  bins in Figure 6. Apparently, the opposite trends in the  $m$ -dependence of  $\varepsilon_c$  and  $\varepsilon'$  counterbalance each other so as to yield a  $\varepsilon$  that depends only weakly on  $m$ .

Our results clearly demonstrate that the environmental effect on centrals has to be taken into account in order to reproduce the  $m$ -independence of the quenching efficiency seen for the total population. This is particularly important for massive centrals. Peng et al. (2012) also found a significant environmental dependence for central galaxies. However, they suspected that it is caused by the misidentification of satellites as centrals. We indeed find some signals for such misidentification in our results. For example, some abnormal behavior of the lowest mass galaxies in high-density bins can be seen in  $\varepsilon_s$ , as well in  $\varepsilon_c$ . More recently, Hirschmann et al. (2014) investigated the misidentification problem using mock galaxy catalogs constructed from a semi-analytic model of galaxy formation, and found that the contamination in centrals is less than 10% for most galaxy masses and environmental densities. The average contamination is less than 6.5%, roughly independent of  $m$  (see also Lange et al. 2017). Since the difference between  $F_{q,c}$  and  $F_{q,s}$  rapidly decreases with increasing  $m$  (Figure 2), the impact of the contamination is expected to decrease with  $m$ . In contrast, the observed  $\Delta$ -dependence is more important for more massive galaxies. Based on these results, we are confident that central-satellite contamination does not significantly impact our conclusion that satellite quenching alone cannot account for the  $m$ -independence of the quenched efficiency, at least for massive galaxies.

An interesting question is why the increase of  $\varepsilon_c$  with increasing  $m$  apparently compensates the decrease of  $\varepsilon'$  with increasing  $m$ . It might reflect some deeper connection between the quenching processes for centrals and satellites. As shown above, the quenched fractions of centrals and satellites of the same stellar mass correlate with the environment as characterized by halo mass in the same way. This suggests that centrals and satellites may experience similar quenching processes which are ultimately related to the host halo mass. In Section 6 we will construct simple models to investigate this issue.

## 5. HALO-BASED QUENCHING EFFICIENCIES

As discussed earlier, halos play a crucial role in shaping galaxy properties. Many quenching processes are thought to correlate with halo mass and stellar mass (see Mo et al. 2010). In order to examine this, we define two new quenching efficiencies in the same vein as the environmental quenching efficiency of Equation (4). These are the halo-based environmental quenching efficiency,

defined as

$$\varepsilon(m, M|M_0) \equiv \frac{F_q(m, M) - F_q(m, M_0)}{1 - F_q(m, M_0)}, \quad (12)$$

and the stellar mass quenching efficiency, defined as (see also Peng et al. 2010)

$$\varepsilon_m(m, M|m_0) \equiv \frac{F_q(m, M) - F_q(m_0, M)}{1 - F_q(m_0, M)}. \quad (13)$$

Here  $M_0$  and  $m_0$  are the halo mass and stellar mass ‘zero-points’ against which the dependencies on  $M$  and  $m$  are compared. Note that  $\varepsilon(m, M|M_0)$  and  $\varepsilon_m(m, M|m_0)$  characterize the dependence on halo mass and stellar mass, respectively, of the combined effect of all quenching processes, including ‘environmental processes’ (such as ram-pressure/tidal stripping and strangulation) and ‘internal processes’ (such as quenching induced by AGN and supernova feedback).

### 5.1. Quenching efficiencies for the total population

Ideally, one would like to adopt the lowest halo mass as ‘zero-point’ environment to calculate the environmental efficiency. However, because no massive galaxy ( $\log(m) > 10.6$ ) resides in halos of  $\log(M) < 12$ , choosing the lowest halo mass bin is inappropriate. We therefore adopt  $13 \leq \log(M) < 13.5$  to define the quenching zero-point, at which the estimates of the quenched fraction are robust for all stellar mass bins (see Figure 3). The corresponding efficiency, obtained from Equation (12), is shown as a function of halo mass in Figure 8. Here again the environmental quenching efficiency is almost independent of stellar mass, although it increases strongly with halo mass. It is easy to see that, if the efficiency is independent of stellar mass, this independence holds regardless of the value of  $M_0$  used. This result clearly shows that the environmental dependence of the quenched fraction can be well separated from the dependence on stellar mass, independent of whether the environmental parameter is the large scale matter density or the mass of the host halo in which the galaxies reside.

Motivated by Equation (5) and that the dependence of  $F_q$  on halo mass can be well described by a power law function (Figure 3), we propose to use a simple formula to describe the quenched fraction:

$$F_q(m, M) = 1 - \exp \left[ - \left( \frac{m}{m_*} \right)^d \right] (a \log M - ac). \quad (14)$$

It results in an environmental quenching efficiency given by

$$\varepsilon(m, M|M_0) = \frac{1}{c - \log M_0} \log \frac{M}{M_0}. \quad (15)$$

We first use Equation (15) with  $\log(M_0) = 13.25$  to fit the data points shown in Figure 8. The best fit gives  $c = 16.37 \pm 0.06$  and is shown as the grey line in Figure 8. We then use Equation (14) to fit the quenched fraction for the total population shown in Figure 3, with  $c$  fixed to 16.37. The best fit values for the other three parameters are  $a = -0.2 \pm 0.004$ ,  $m_* = 6.5 \pm 0.2 \times 10^{10} h^{-2} M_\odot$  and  $d = 0.61 \pm 0.02$ .

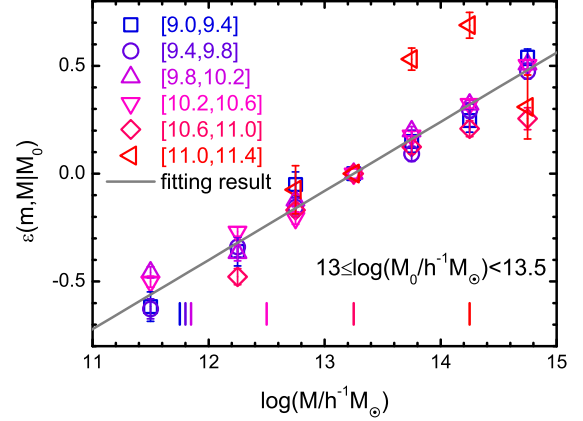


FIG. 8.— The symbols with error bars show the environmental quenching efficiency  $\varepsilon(m, M|M_0)$  [see Equation (4)] as a function of halo mass  $M$  for galaxies of different masses, as indicated in the panel. The efficiency is calculated by using galaxies with  $13 \leq \log M_0/M_\odot < 13.5$  to estimate  $F_q(m, M_0)$ . The gray line is the fitting curve (Equation 15) of the data. The short vertical lines mark the halo masses at which galaxies in a given stellar mass bin transit from central dominated to satellite dominated.

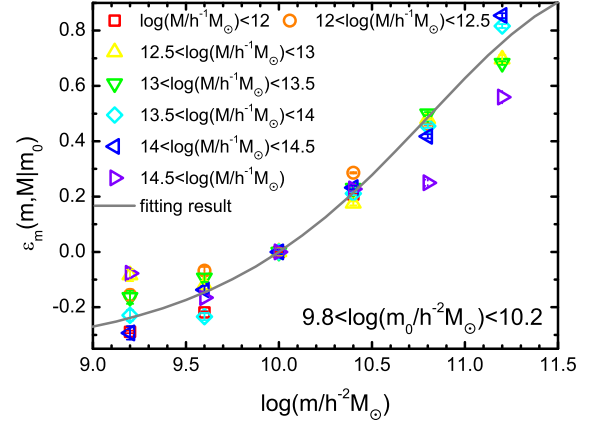


FIG. 9.— The symbols with error bars show the mass quenching efficiency  $\varepsilon_m(m, M|m_0)$  [see Equation (13)] as a function of stellar mass  $m$  for different halo masses, as indicated in the panel. The efficiency is calculated by using galaxies with  $9.8 \leq \log m_0/h^{-2}M_\odot < 10.2$  to estimate  $F_q(m_0, M)$ . The gray line is the fitting curve (fitting formula Equation 16).

The results for  $\varepsilon_m(m, M|m_0)$  are presented in Figure 9. Here we choose  $9.8 \leq \log m_0 < 10.2$  so that we have robust estimation of  $F_q(m_0, M)$  for all the halo-mass bins. As one can see, the  $\varepsilon_m(m, M|m_0) - m$  relation is quite independent of halo mass in all the halo mass bins except the most massive halo bin. Since the quenched fraction can be well fitted by Equation (14),  $\varepsilon_m(m, M|m_0)$  can be described by

$$\varepsilon_m(m, M|m_0) \equiv 1 - \exp \left[ - \left( \frac{m}{m_*} \right)^d + \left( \frac{m_0}{m_*} \right)^d \right]. \quad (16)$$

The prediction of this equation with  $m_* = 6.5 \times 10^{10} h^{-2} M_\odot$ ,  $d = 0.61$  and  $m_0 = 10^{10} h^{-2} M_\odot$  is plotted as the grey line in Fig. 9.

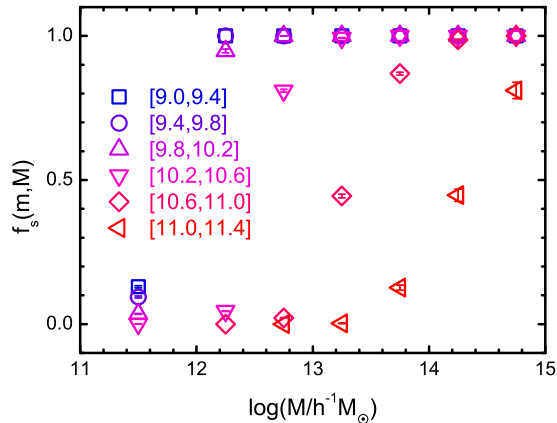


FIG. 10.— The symbols show satellite fraction as a function of halo mass in various stellar mass bins.

### 5.2. Quenching efficiencies for centrals and satellites

As shown in Sections 4.2 and 4.3, the density-based quenching efficiencies for central and satellite populations depend on stellar mass in an opposite way, and they counterbalance each other to produce a  $m$ -independent efficiency for the total population. It is thus also interesting to examine the quenching efficiencies for centrals and satellites separately by using halo mass, instead of the density, as the environmental parameter. However, we will not repeat the same analyses as in Section 4.2 and 4.3, for the following two reasons. First, the stellar masses of centrals are strongly correlated with the halo masses of their host groups, so that it is difficult to find a single halo mass bin to define the environmental zero point for central galaxies of different masses. Second, for satellites with given  $(m, M)$ , it is difficult to select a large number of centrals of the same  $(m, M)$  to form a control sample to calculate the satellite-specific quenching efficiency. Because of these we adopt a different approach, as described below.

To start with, we look at the satellite fraction as a function of halo mass in different stellar mass bins, as shown in Figure 10. Unlike the smooth relation between the satellite fraction with  $\Delta$  shown in Figure 7,  $f_s(m, M)$  as a function of  $M$  resembles roughly a step function, particularly for low-mass galaxies. The fraction is close to zero at  $M < M_{\text{tr}}$  and about one at  $M > M_{\text{tr}}$ , where  $M_{\text{tr}}$  is the mass scale at the transition of the step function and increases with increasing stellar mass. Therefore, centrals and satellites dominate the galaxy population in different regions in the  $(m, M)$  plane and the two populations are comparable in number only in a narrow region in the  $(m, M)$  plane. This property of the satellite fraction can be used to understand the quenching efficiency of centrals and satellites over a large range in  $m$  and  $M$ .

As shown in Figure 8,  $\varepsilon(m, M|M_0)$  for galaxies of a given  $m$  follows the same correlation with  $M$  below and above  $M_{\text{tr}}(m)$  (marked by the vertical lines in the figure), where galaxies are dominated by centrals and satellites, respectively. This indicates that the quenched fractions in both the central and satellite populations depend on the host halo mass in a similar way not only in the  $M$  range where the two populations overlap, but

also over the whole  $M$  range. Similar analysis can also be performed on the basis of the mass quenching efficiency  $\varepsilon_m$ . For example, the four stellar mass bins in  $9.0 < \log(m) < 10.6$  are all dominated by centrals in halos with  $\log(M) < 12$ , but by satellites at  $\log(M) > 13$ . However, the mass quenching efficiency follows the same trend with stellar mass in different halo mass bins, no matter whether the galaxies in the halo mass bin are dominated by centrals or by satellites. All these suggest that, whatever the quenching processes are, they tend to produce a quenching efficiency that depends on halo and stellar masses in a similar way for both centrals and satellites. The results also suggest that the similarity in quenching efficiency between centrals and satellites exists not only in the region of the  $(m, M)$  plane where the two populations overlap, but also over the whole range of  $(m, M)$  covered by the sample.

## 6. HALO MASS AND ASSEMBLY DRIVE ENVIRONMENTAL QUENCHING

As we have shown above, the quenched fraction of galaxies depends on both halo mass and environmental density. It is therefore important to examine whether it is the halo mass or the environmental density that plays the dominating role. To address this question, we construct two simple models, in which the quenched fraction is assumed to be determined by the stellar mass combined with one of the two environmental quantities. We also try to understand whether assembly histories of dark matter halos affect the galaxy properties in a third model. These models will also help us to understand the apparent discrepancy between the results based on environmental density and halo mass. Namely why is the density-based quenching efficiency independent of the stellar mass for the total population but stellar-mass dependent when centrals and satellites are analyzed separately (Section 4), while centrals and satellites follow very similar trends in the halo-based quenching efficiency (Section 5)?

In the first model (hereafter Model A), the environmental density,  $\Delta$ , is assumed to be the primary driver of the environmental dependence of quenching. For each real galaxy in our SDSS sample, we construct a corresponding model galaxy, which has exactly the same  $m$ ,  $M$ ,  $\Delta$ , and the same identification as either a central or a satellite. We assign a given model galaxy  $i$  a quenching probability,  $q_i = F_q(m, \Delta)$ , according to its position in the  $(m, \Delta)$  space (Figure 2). Note that centrals are treated differently from satellites, because the observed  $F_{q,c}(m, \Delta)$  is very different from  $F_{q,s}(m, \Delta)$ . We then use Equation (3) to estimate the average quenched fraction for any given subset of the model galaxies. Figure 11 shows the predicted quenched fraction as a function of halo mass,  $M$ , for galaxies in different  $m$  bins.

As one can see, Model A predicts a positive dependence of the quenched fraction on  $M$ , in rough agreement with the observation. This dependence is expected from the fact that dark matter halos are tracers of the matter density field. Note, however, that there is a marked difference between the model prediction and the observational data. First of all, the model predicts no significant dependence of  $F_{q,c}$  on  $M$ , contrary to the data which reveals a clear trend of increasing  $F_{q,c}$  with increasing  $M$  (cf., Figure 3). Second, the predicted  $M$ -dependence for

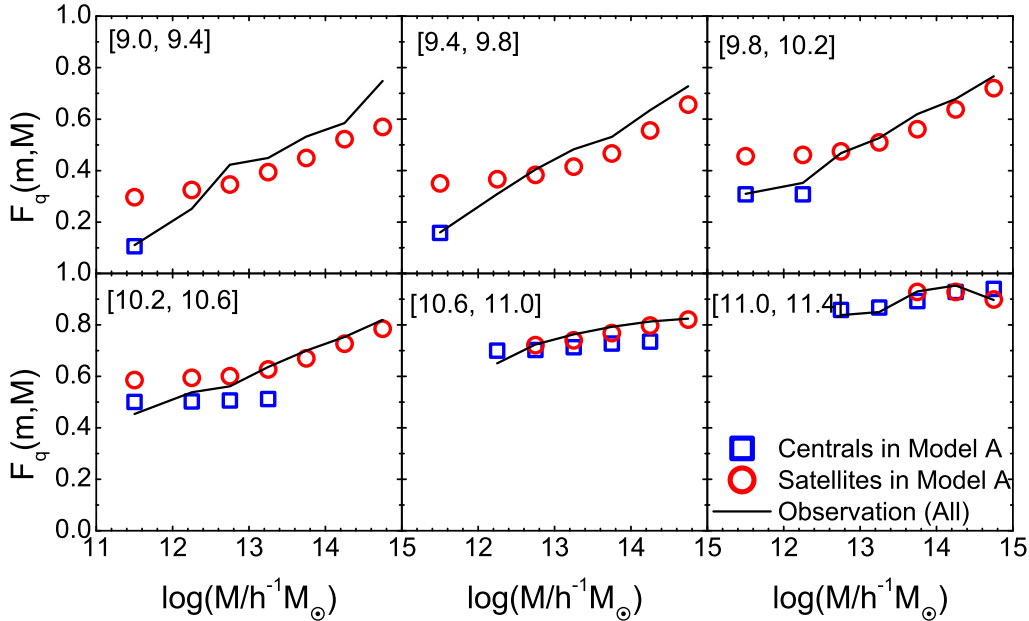


FIG. 11.— Similar to Figure 3 but for Model A. The model results for the central (squares) and satellite (circles) populations are plotted separately. The black lines show the observational results for the total population.

satellite galaxies is also weaker than observed. This discrepancy is particularly large for low mass galaxies in low mass halos, where the model overpredicts  $F_{q,s}$  by as much as 0.2. Finally, the model predicts significant differences between the quenched fractions of centrals and satellites of similar  $m$  and  $M$ , while such differences are absent in the observational data (cf., Figure 3).

In the second model (hereafter Model B), halo mass instead of environmental density is assumed to be the primary driver of the observed environmental dependence of quenching. To test this hypothesis, we construct a model galaxy sample by assigning each real galaxy in our SDSS sample a quenching probability  $q_i = F_q(m, M)$  based on its position in the  $(m, M)$  plane (the black solid lines in Figure 3). Since the dependence of  $F_q$  on  $M$  and  $m$  is very similar between centrals and satellites, we do not distinguish between them when assigning  $q_i$ . Hence, in this model the probability for a galaxy to be quenched is solely determined by the galaxy’s stellar mass and host halo mass, with centrals and satellite being treated in exactly the same way.

The quenched fractions predicted by Model B as a function of  $\Delta$  and  $m$  [computed using Equation (3)] are shown in Figure 12. The results closely resemble those for the real galaxies. To better illustrate the quality of the model, Figure 13 plots the differences between the model prediction and the data,  $\delta F_q(m, \Delta)$ . Note that the differences are fairly small, typically less than  $\sim 0.05$  for the entire galaxy sample. For centrals the discrepancies are slightly larger, while for satellites the differences are comparable to the observational uncertainties. Hence, Model B provides a fairly accurate description of the data. Taken together, the results from Models A and B strongly suggest that the mass of the host halo is a far more important environmental parameter for regulating quenching than is the matter density.

Before moving on, we try to understand some of the general trends predicted by Model B. The resulting dependence of  $F_q$  on  $\Delta$  is very different for centrals and satellites, although the two populations are assumed to have exactly the same dependence of  $F_q$  on  $m$  and  $M$ . This arises because centrals and satellites of a given  $m$  cover very different ranges in  $M$ . Centrals with  $9 \leq \log(m) \leq 10.2$  usually reside in halos with  $\log(M) \sim 12$ . The halo bias at this mass scale is close to unity with little dependence on  $M$  (see Sheth, Mo & Tormen 2001). Hence, the mean halo mass in the low-density regions is not very different from that in the high-density regions, which explains why  $F_{q,c}$  is almost independent of  $\Delta$  for galaxies in this  $m$  range. As the mass of the central galaxy increases, so does the mass of its host halo, which pushes it into the regime where halo bias is larger than unity and has a strong dependence on halo mass. Consequently, halos in high density regions are, on average, more massive than those in low density regions, even if they contain centrals of the same stellar mass. This explains why the dependence of  $F_{q,c}$  on  $\Delta$  becomes stronger for centrals with higher stellar masses, as shown in Figure 12. However, for a given  $m$ , the distribution in  $M$  is quite narrow (see Yang et al. 2009), so the  $\Delta$ -dependence predicted by Model B remains weak. For satellites, the situation is very different. At the low  $m$  end, satellites reside in halos that cover a very wide range in  $M$ , which gives rise to a very strong dependence on  $\Delta$ . As  $m$  increases, the dispersion in  $M$  decreases, which weakens the dependence of  $F_{q,s}$  on  $\Delta$ .

As evident from Figure 13, Model B slightly overestimates  $F_{q,c}$  at the low- $\Delta$  end while underestimating it at the high- $\Delta$  end, a trend that is evident for every stellar mass bin. It suggests that the quenching of (central) galaxies depends not only on halo mass and stellar mass, but also on some other halo properties that are correlated

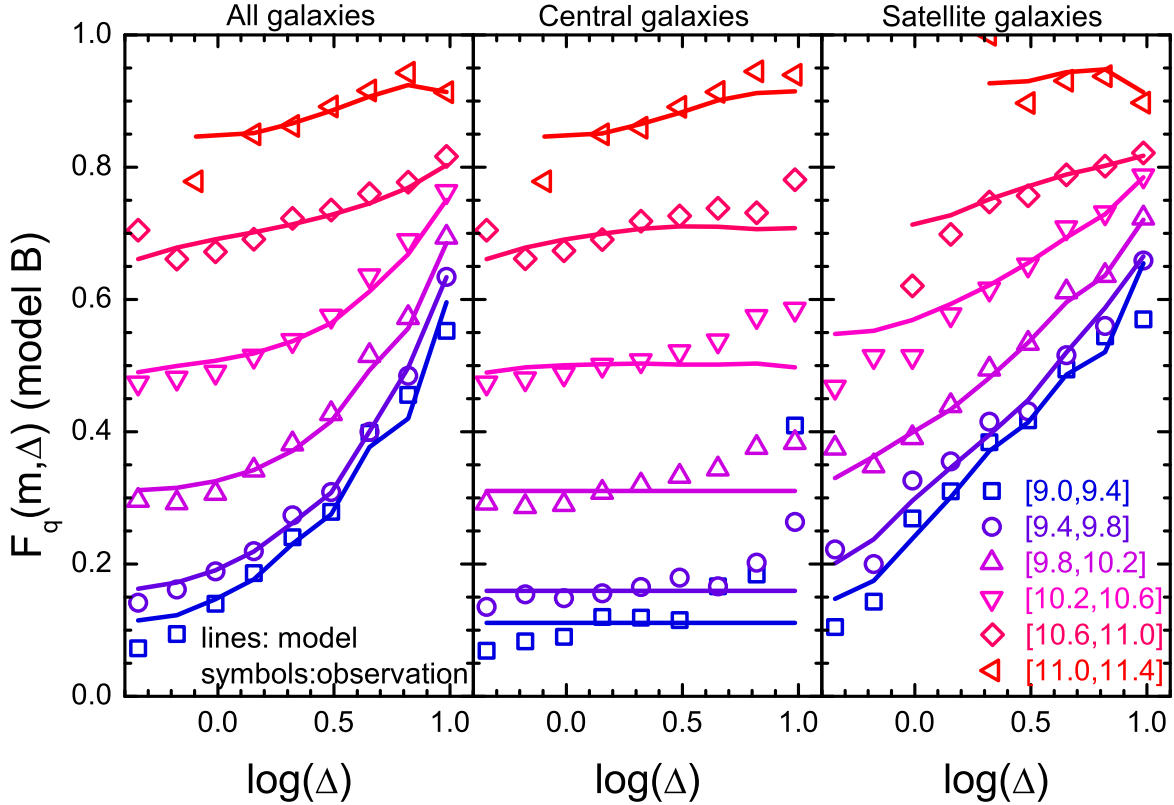


FIG. 12.— Similar to Figure 2 but obtained from Model B. The model results are shown in lines. The symbols show the corresponding observational results (exactly the same as that in Figure 2).

with the environmental density. One such halo property is halo assembly history, which is correlated with the environmental density (known as assembly bias). In order to see if the discrepancy can be explained by halo assembly bias, we need to know, for each individual group, the formation redshift (hereafter  $z_f$ ) that characterizes its assembly history. Our ELUCID simulation is a constrained simulation in the SDSS DR7 region and can reliably reproduce most of massive groups (see paper III), and here we make use of the information it provides to estimate the formation redshifts for individual groups. To do this, for each group, we search all halos in the simulation that have mass differences less than 0.3 dex with, and distance less than  $5 h^{-1} \text{Mpc}$  to, the group in question. Most of the groups ( $\sim 97.4\%$ ) have at least one halo companion defined in this way, and we assign the formation redshift of the nearest halo to the group. The formation redshift is defined as the highest redshift at which half of the final halo mass has assembled into progenitors more massive than  $10^{11.5} h^{-1} M_\odot$  (see Neistein, van den Bosch & Dekel 2006; Li et al. 2008). The choice of this mass limit is motivated by the fact that it corresponds to the halo mass at which the star formation efficiency is the highest at different redshifts (see Lim et al. 2017). For groups with  $\log(M) < 12.0$  that do not have accurate halo mass estimates in the group catalog, we only search for halo companions with  $11.7 < \log(M) < 12.0$ , where the lower mass limit (11.7) is adopted so that all halos have reliable estimates of halo formation redshifts in the ELUCID simulation. We have also used other definitions

of halo formation redshift, such as the redshift at which the main progenitor reaches half of the present-day halo mass. The results are very similar.

A third model, Model C, is then constructed on top of Model B. In Model C, the quenching probability of a model galaxy depends not only on  $m$  and  $M$ , but also on the formation redshift of its halo. The simplest way to link  $z_f$  to quenching probability is to assume that a galaxy is quenched when  $z_f > z_{\text{th}}$ , where  $z_{\text{th}}$  is a formation redshift threshold. In reality, however, galaxies with given  $z_f$ ,  $m$  and  $M$ , must have some dispersion in their star formation rate. To mimic this, we introduce a dispersion in  $z_f$  for each system before applying the criterion  $z_f > z_{\text{th}}$  to select the quenched fraction. In practice, for a galaxy  $i$  with  $z_f = z_f^i$ , we use a Monte Carlo method to generate 500 mock galaxies, with their formation redshifts ( $z_{f,m}^i$ ) randomly drawn from a Gaussian distribution with the mean value equal to  $z_f^i$  and a width  $\sigma_z$ . Then, for a given  $z_{\text{th}}$ , the quenching probability of the model galaxy,  $q_i$ , is set to be the fraction of the mock galaxies that have  $z_{f,m}^i > z_{\text{th}}$  among the 500 mock galaxies. In order to introduce the dependence on  $m$  and  $M$ , the threshold  $z_{\text{th}}$  is required to be a function of the two quantities, and is determined by the criterion that the dependence on  $m$  and  $M$  for the model galaxies is exactly the same as that for real galaxies. Note that in our model the formation redshift dependence is only considered for central galaxies; satellites are treated in exactly the same way as in Model B.

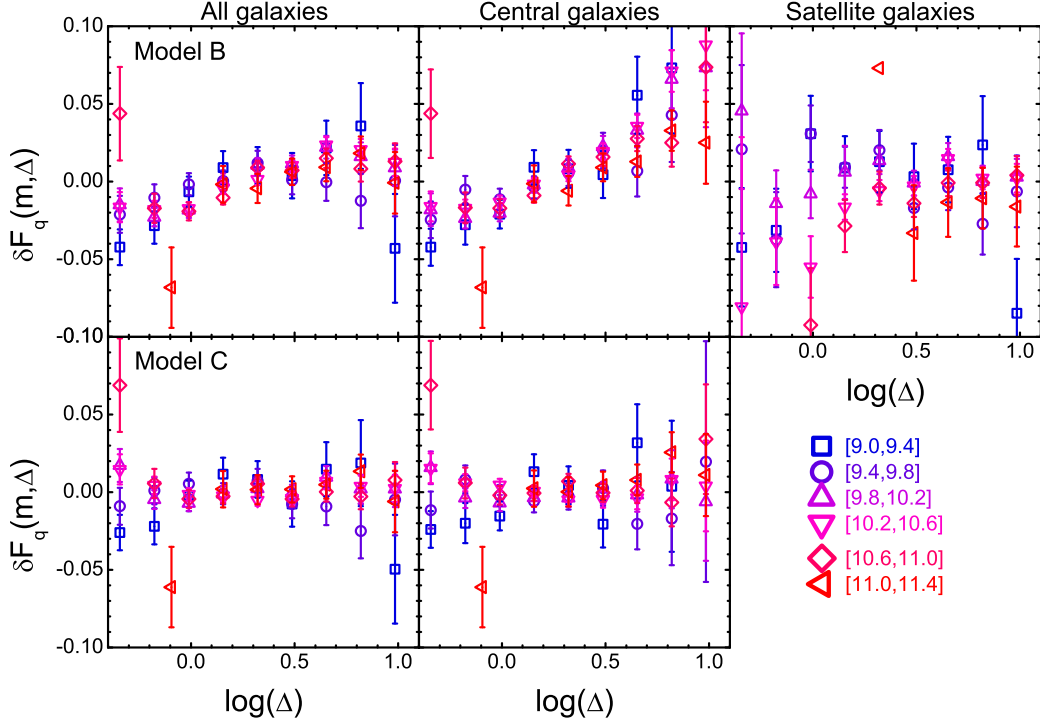


FIG. 13.— The difference in the quenched fraction between the observation results and model predictions (upper panels: Model B; lower panels: Model C). The results for satellites are the same between the two models. The uncertainties are the error bars from the observational data, as shown in Figure 2. The uncertainties in models are not taken into account.

When  $\sigma_z$  is set to be 0, the dependence of  $F_{q,c}(m, \Delta)$  on  $\Delta$  for the model galaxies is found to be much stronger than that for real galaxies. We have experimented a series of values for  $\sigma_z$ , and found that the model matches the observation the best when  $\sigma_z \sim 0.8$ . Figure 14 shows the quenched fraction as a function of  $m$  and  $\Delta$  obtained from this best model. A significant increasing trend of the quenched fraction with  $\Delta$  is now produced for central galaxies in most of  $m$  bins, as is seen in the observational data. The lower two panels of Figure 13 show the difference between the observational quenched fraction and the predictions of Model C for the total population and centrals, respectively. In contrast to Model B, the dependence of  $\delta F_q(m, \Delta)$  on  $\Delta$  almost completely disappear in Model C.

We then compute the environmental quenching efficiency, defined in Equation (4) with the zero point estimated from data at  $\log \Delta \leq 0$ , for Model B and C. The results are presented in the left panels of Figure 15. The quenching efficiency predicted by Model B exhibits a very weak dependence on  $m$ . This is not surprising since the halo-based environmental efficiency,  $\varepsilon_c(m, M|M_0)$ , is independent of stellar mass (Figure 8) and since halo mass is the only driver of the environmental quenching in Model B. There is a small deviation between the model prediction and the observation for most of the stellar mass bins. Such deviation is absent in Model C, suggesting that it has the same origin as that shown in Figure 13.

We also show the predictions of Model B and C for  $\varepsilon_c(m, \Delta|\Delta_0)$ , defined by Equation (7), and for

$\varepsilon'(m, \Delta|\Delta_0)$ , defined by Equation (10), in the middle and right panels of Figure 15. In Model B, one can see a clear trend that, at a fixed  $\Delta$ ,  $\varepsilon_c$  increases, while  $\varepsilon'$  decreases, with  $m$ . As discussed above, the halo mass distribution becomes broader for centrals but narrower for satellites as stellar mass increases, which explains the opposite trends in the quenched efficiency as a function of stellar mass for centrals and satellites. After taking into account the assembly bias effect (Model C), the dependencies on stellar mass for both centrals and satellites are enhanced and the predictions resemble more closely the observational results.

Moreover, the predicted efficiency for the most massive galaxies is now closer to the other mass bins than the observational result, giving further support to the hypothesis that the discrepancy found for the most massive galaxies in the observational data is mainly caused by the uncertainty in the estimation of  $F_q(m, \Delta_0)$ . The uncertainty is largely eliminated in the model predictions, because the value of  $q_i$  assigned to galaxies in the low-density regions is the average over a larger sample of galaxies.

## 7. THE QUENCHING OF CENTRALS IS NOT SPECIAL

As shown in Section 3.3 and 5.2, we find that centrals and satellites follow the same correlation of quenched fraction with stellar mass and host halo mass. This result appears to be in conflict with those obtained by some earlier studies (e.g. van den Bosch et al. 2008; Wetzel et al. 2012; Peng et al. 2012), where quenching is found to depend strongly on whether a galaxy is a central or

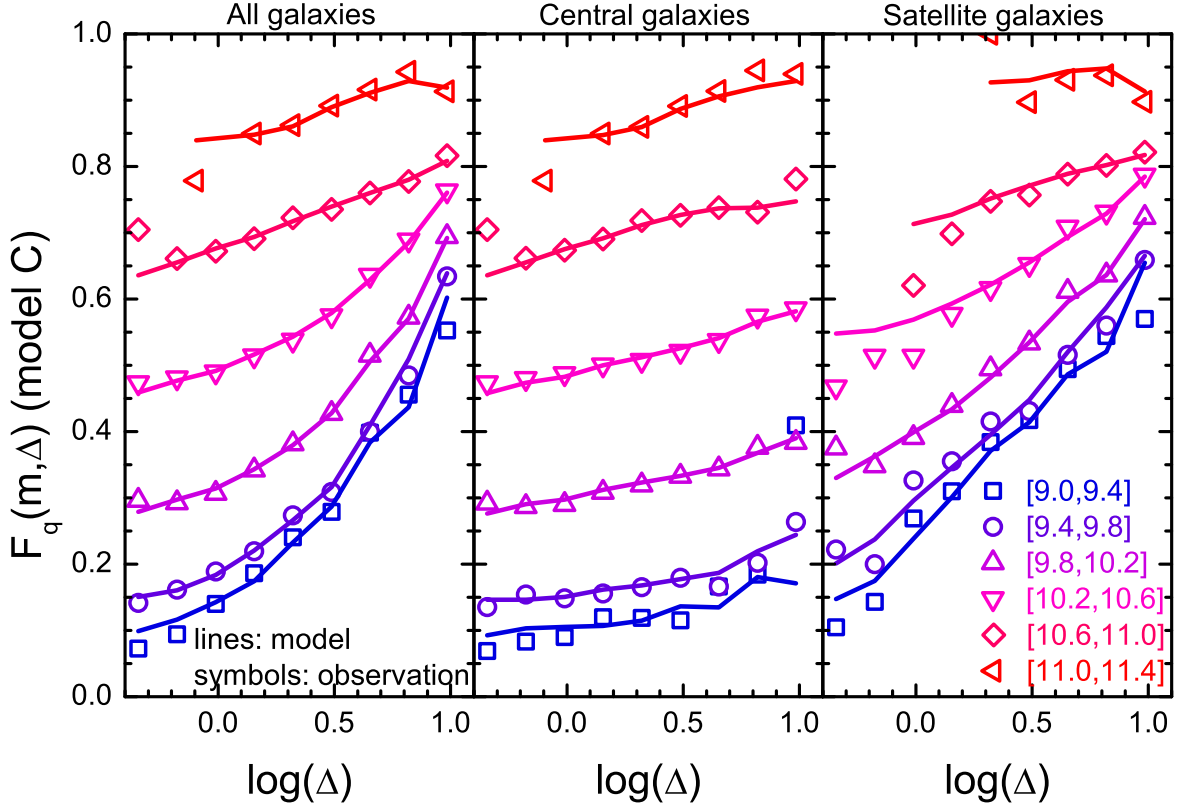


FIG. 14.— Similar to Figure 2 but obtained from Model C. The model results are shown in lines. The symbols show the corresponding observational results (exactly the same as that in Figure 2).

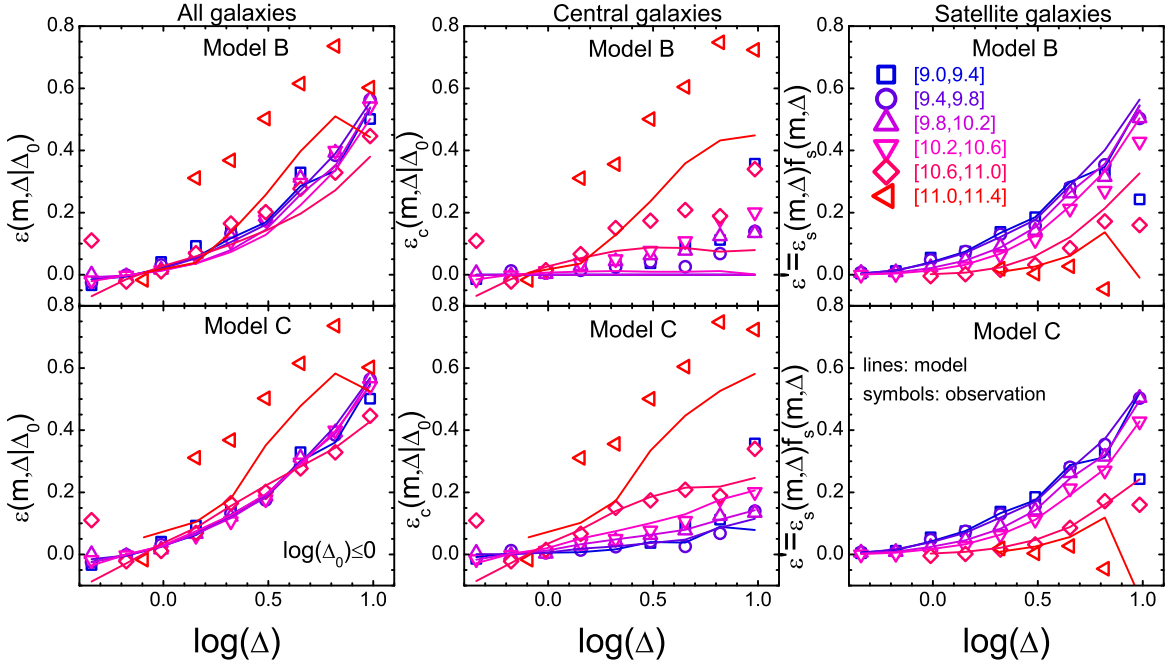


FIG. 15.— The environmental quenching efficiencies for model B (upper panels) and model C (lower panels). Lines show the model prediction and symbols show the corresponding observational data. Left panels: efficiency of Equation (4). Middle panels: efficiency of Equation (7). Right panels: efficiency of Equation (10). For the most massive galaxies in Model C and in the observational data, the data point at  $\Delta \sim 1.0$  lies outside the figure boundary.

a satellite. However, as discussed above, host halo mass ranges covered by centrals and satellites of the same stellar mass are very different. Thus, if halo mass is not used as a control parameter when comparing the two populations, as is the case in most of the previous studies, then one is comparing centrals in low mass halos with satellites in massive ones and neglecting the strong dependence on halo mass. We believe that this is the origin of the discrepancy and that there is no conflict between our results and those obtained in these earlier studies.

It is possible that the similarity between centrals and satellites we find in the data is not real, but caused by errors in the group finder used to identify groups and central galaxies in them. As one can see from Figure 10, the satellite fraction,  $f_s(m, M)$ , resembles roughly a step function and is close to zero at  $M < M_{\text{tr}}$  and about one at  $M > M_{\text{tr}}$  ( $M_{\text{tr}}$  is the mass scale at the transition of the step function). Thus, even if the mis-identification fraction is small in the whole population (see Hirschmann et al. 2014), the galaxies that are identified as satellites at  $M < M_{\text{tr}}$  may be significantly contaminated by centrals. In this case, the similarity between centrals and ‘satellites’ of a given stellar mass in their quenched fraction may be produced by the false identification between centrals and satellites, rather than a real similarity.

However, it is difficult to explain the  $m$ -independence of the environmental quenching efficiency and the  $M$ -independence of the stellar mass quenching efficiency (Section 5) by central/satellite mis-identifications alone. If centrals and satellites had quenching properties that depend on the halo and stellar masses in significantly different ways, the environmental quenching efficiency,  $\varepsilon(m, M|M_0)$ , would be expected to correlate with the halo mass in different ways depending on whether  $M < M_{\text{tr}}$  or  $M > M_{\text{tr}}$ , as the galaxy populations in the two mass ranges are dominated by centrals and satellites, respectively (see Fig. 10). Moreover, since  $M_{\text{tr}}$  increases with increasing stellar mass,  $\varepsilon(m, M|M_0)$  would also be expected to vary with stellar mass. Similarly, it would also lead to  $M$ -dependence in the mass quenching efficiency,  $\varepsilon_m(m, M|m_0)$ . Both are inconsistent with the observational results. We thus conclude that the similar quenching properties of centrals and satellites are not produced by mis-identifications between the two populations, and are real within the statistical uncertainties of the data.

It should be pointed out that this interpretation is based on the premise that the inferred halo mass is sufficiently accurate. Recently, Campbell et al (2015) used a mock catalog including galaxy color to check the color-dependent statistics inferred from group catalogs. They compared the marginalized dependence of the quenched (red) fraction on halo mass obtained from their mock group catalog with that obtained directly from the simulation used to construct the mock catalog, and found that group finders tend to reduce the difference in the quenched fraction between centrals and satellites (see their figure 13). This systematic error is produced by the combined effect of group membership determination, central/satellite designation, and halo mass assignments. If the real difference between centrals and satellites is small, it may be washed out by this error. However, we want to point out that if this systematic error shown in the mock group catalog in Campbell et al. indeed af-

fects the SDSS group catalog in a similar way, one would expect to see that the marginalized dependence of the quenched fraction on halo mass is similar between centrals and satellites for the SDSS group catalog. It is apparently inconsistent with what we found (the middle panel of Figure 1). This suggests that the error caused by group finder depends on the galaxy formation model that is used to construct the mock catalog. Unfortunately this also means that the impact of the inaccuracy of the group finder on the results obtained here from the SDSS group catalog is unclear.

One way to bypass the uncertainty in the central versus satellite identification is to study the dependence of galaxy quenching on the locations of galaxies in their host halos. Instead of looking at centrals versus satellites, we can look at galaxies at different locations in a halo. By definition, centrals belong to the innermost population. Previous studies (e.g. Wetzel et al. 2012; Woo et al. 2013; Bluck et al. 2016) found that the quenched fraction increases with decreasing distance to the halo center (halo-centric radius). In contrast, the similarities between centrals and satellites found in this paper seem to suggest that quenching is quite independent of the location within halos. To find the cause of this discrepancy, we divide the total galaxy population into two: the inner and outer sub-populations, according to whether or not their projected distances to the halo centers ( $R_p$ ) are smaller or larger than half of the virial radii ( $R_{\text{vir}}$ ). Here the center of a halo is the luminosity-weighted position of its member galaxies. Figure 16 shows the quenched fraction as a function of stellar mass for the two sub-populations in the six halo mass bins used above. To compare with the central galaxies in the corresponding halo mass bin, the quenched fraction is scaled with the quenched fraction of centrals and the stellar mass is also scaled with the median of the stellar mass of central galaxies ( $\tilde{m}_c$ ). For comparison, the satellite fractions in the two sub-populations are also shown in the figure.

For small galaxies, the quenched fraction clearly increases with the decrease of halo-centric radius, consistent with previous studies, while for massive galaxies the dependence on halo-centric radius is very weak. The characteristic stellar mass above which the  $R_p$  dependence becomes weak is  $\log m \simeq \log(\tilde{m}_c) - 0.7$  (indicated by the vertical lines) and almost independent of halo mass. This clearly demonstrates that the quenching probability is independent of its location in the halo, as long as a galaxy has a stellar mass larger than about one fifth of the mass of its central galaxy. For galaxies with  $\log m \sim \log \tilde{m}_c$ , the scaled quenched fraction is close to unity for both the inner and outer populations. At this stellar mass, the satellite fraction is close to zero for halos with  $\log(M) < 12.5$  and increases to  $> 60\%$  for  $\log(M) > 14.5$ . It indicates that, when galaxies have stellar masses comparable to those of their centrals, the quenched fraction is the same as that of their centrals, no matter where they are located and whether they are identified as centrals or not. Alternative separations of inner and outer regions at  $0.3R_{\text{vir}}$  and  $0.4R_{\text{vir}}$  have no significant impact on this conclusion. These demonstrate again that centrals are not special as far as their quenching properties are concerned. Our results are also not in conflict with previous finding, as a strong dependence on halo-centric radius is present but only for galaxies that

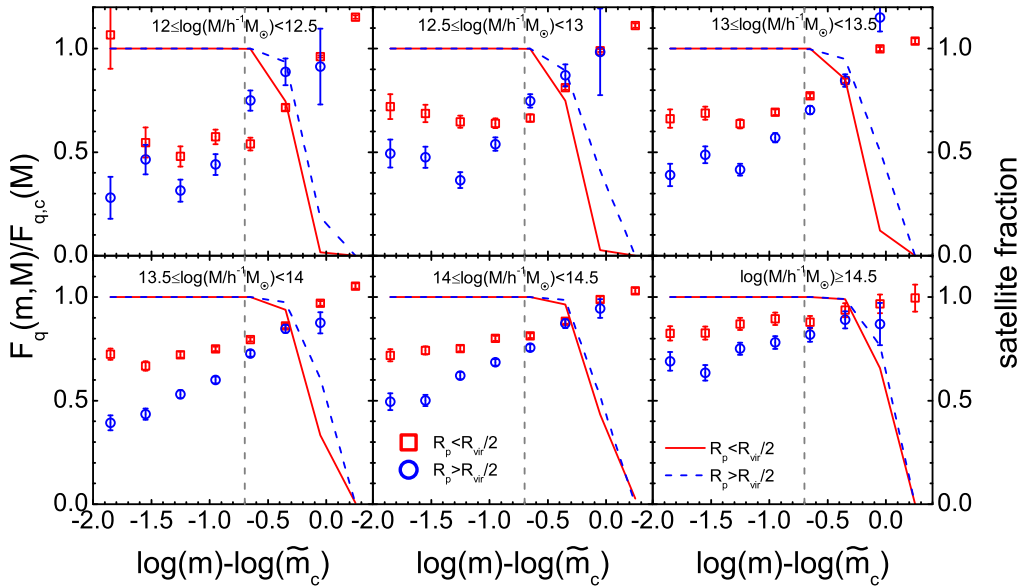


FIG. 16.— The symbols show the scaled quenched fraction as a function of the scaled stellar mass for galaxies with  $R_p < R_{\text{vir}}/2$  (red squares) and  $R_p > R_{\text{vir}}/2$  (blue circles) in six halo mass bins. The red and blue lines show the satellite fraction as a function of scaled stellar mass. The vertical dashed lines indicate  $\log(m) - \log(\tilde{m}_c) = -0.7$ . Here the quenched fraction,  $F_q(m, M)$ , is scaled by  $F_{q,c}(M)$ , the quenched fraction of central galaxies in the corresponding halo mass bins, and the stellar mass is scaled with  $\tilde{m}_c$ , the median of the stellar mass of central galaxies.

are much less massive than the centrals in their corresponding halos.

## 8. SUMMARY AND DISCUSSION

In this paper, we present a detailed investigation about the environmental dependence of quenching of star formation using a large sample of galaxies constructed from the SDSS. We adopt two quantities to describe the different aspects of galaxy environments: the environmental mass densities, smoothed on a scale of  $4 h^{-1} \text{Mpc}$  (half width of Gaussian kernel) at the positions of individual galaxies, and the masses of the host halos within which galaxies reside. The mass densities are obtained from the ELUCID simulation, a constrained  $N$ -body simulation in the SDSS volume, while the halo masses are based on a galaxy group catalog constructed with a halo-based group finder. Our main findings are summarized as follows.

- The quenched fraction of galaxies increases systematically with galaxy stellar mass, environmental density and host halo mass. When analyzed separately, centrals and satellites show very different density-dependence: while the dependence is strong for satellites, it is weak or even absent for central galaxies. The environmental effect is stronger for centrals with higher stellar masses, while satellites show the opposite trend. In contrast, the dependence of the quenched fraction on halo mass is almost the same for both centrals and satellites, although the two populations cover different ranges of halo masses.
- For the total galaxy population, the quenching efficiency, defined as the quenched fraction of galax-

ies in a given environment relative to a zero-point population, is found to be almost independent of galaxy stellar mass over a wide mass range,  $9 \leq \log(m) \leq 11.4$ , no matter which environmental parameter (mass density or halo mass) is adopted. This suggests that the strong stellar mass-dependence of the quenched fraction is predominantly produced by such a dependence of the zero point.

- When central and satellite galaxies are analyzed separately, the density-based quenching efficiency is found to increase systematically with stellar mass for centrals but to decrease for satellites, and the stellar mass dependence is stronger for galaxies of higher stellar masses. The opposite trends seen in centrals and satellites compensate each other so as to make an almost stellar mass-independent quenching efficiency for the total population described above. The results thus do not support the hypothesis proposed in previous studies that the mass independence of the quenching efficiency is only due to satellite quenching.
- Centrals and satellites are found to follow the same trends in both the halo mass and stellar mass based quenching efficiencies, contrary to the efficiency defined by the environmental density. It indicates that quenching does not depend strongly on the location within halo, at least for galaxies with stellar masses comparable to those of the centrals. Further investigation of the dependence of the quenched fraction on the distance to halo center shows that the distance dependence is only important for galaxies with stellar masses that are lower

than one fifth of the masses of their centrals but insignificant for more massive galaxies.

- A model, in which the quenching probability of a galaxy is assumed to be determined by the galaxy stellar mass combined with the host halo mass (Model B), can well reproduce the observed dependence of the quenched fraction on environmental density for the total population, as well as separately for centrals and satellites. In contrast, a model in which the quenching probability is assumed to be determined by galaxy mass and environmental density (Model A) predicts too weak dependence on halo mass and different halo-mass dependence between centrals and satellites, in conflict with observation. These suggest that halo properties are the driver of the environmental quenching seen in the observational data.
- Model B is found to slightly overestimate the quenched fraction in the low density end and to underestimate it at the high density end for central galaxies. It suggests that galaxy quenching depends not only on halo mass but also on some other halo properties that are correlated with the environmental density. A model (Model C), which takes into account halo assembly bias, can explain the discrepancy between Model B and the observational results.
- The environmental quenching efficiency based on the mass density predicted by both Model B and Model C (where the halo-mass is the primary driver of the environmental effect) is found to be independent of stellar mass, consistent with observational results. This strongly suggests that the stellar mass independence of the density-based efficiency originates from the stellar mass independence of the halo-based efficiency.
- The difference in star formation quenching between centrals and satellites found in this paper and in numerous previous studies are mainly due to the difference in the host halo mass ranges covered by the two populations, and not produced by the difference in the correlation of quenching probability with halo mass between the two populations.

Many mechanisms of quenching star formation in galaxies have been proposed in the literature, such as virial shock heating to accretion flows, the feedback from active galactic nuclei and supernova, and the stripping of hot and cold gas associated with galaxies (see e.g. Gabor et al. 2010 for a more comprehensive discussion). The strengths of these quenching mechanisms depend on stellar mass and halo mass in different ways. Furthermore, because of the special positions assumed for central galaxies in their halos, some of the processes may have different impact between centrals and satellites. In what follows we discuss how our findings can be used to constrain these different quenching mechanisms.

AGN feedback has been proposed to quench cooling flows in massive halos and suppress star formation in massive galaxies (e.g. Croton et al. 2006; Bower et al. 2006; Cui, Borgani, & Murante 2014). The strength of

AGN feedback is usually assumed to be more efficient for more massive galaxies that contain more massive black holes in more massive halos. AGN feedback may thus be able to produce the positive dependency of the quenched fraction and quenching efficiency on galaxy stellar mass and halo mass found in this paper. Moreover, AGN feedback may affect both centrals and satellites in a similar way, again consistent with our observation. Numerous observations have provided evidence for AGN feedback through radio jet and massive outflows driven by radiation pressure (e.g. Best et al. 2007; Wang et al. 2011b; Fabian et al. 2012). However, the details how AGN feedback is coupled with the gas and regulates the star formation in galaxies are still uncertain.

Hydrodynamical simulations (e.g. Kereš et al. 2005; 2009) have revealed that galaxies acquire their baryonic mass primarily through cold gas flows along filamentary structures around halos, and such cold accretion can be heated and suppressed by virial shocks in the host halo (see also Dekel & Birnboim 2006). This process can result in a decrease in the cold accretion as a function of halo mass, as radiative cooling is less effective in more massive halos (Ocvirk, Pichon & Teyssier 2008; Kereš et al. 2009). If the star formation in galaxies is fuelled mainly by the cold accretion, an increasing trend of the quenched fraction and the quenching efficiency with halo mass is expected. Moreover, galaxies in simulations are found to continue to acquire cold gas after becoming satellites, and the cold accretion is also affected by the shock in the host halos (Kereš et al. 2009), which is consistent with our finding that the quenching properties of centrals and satellites are similar. Unfortunately, it is unclear how the suppression of cold accretion depends on the stellar mass of a galaxy in a halo, and so it is unclear if this mechanism can accommodate the dependence of quenching on stellar mass seen in the observation.

The stripping of gas from galaxies by ram-pressure in hot halo is expected to be more efficient for galaxies of lower masses living in higher mass halos (see Henriques et al. 2016 for discussion). Therefore this mechanism predicts that quenching should be important only in massive halos with hot halo gas, and that the quenched fraction and quenching efficiency should increase with decreasing stellar mass. These predictions seem to be at odds with the positive dependence of the quenched fraction (quenching efficiency) on stellar mass found in this paper, and with the fact no characteristic halo mass is seen in the quenching fraction - halo mass relation. In addition, ram pressure stripping is expected to be important only for satellite galaxies that are orbiting in halos, but unimportant for centrals that sit close to the bottoms of the halo gravitational potential wells. If such stripping process dominates quenching of star formation, then centrals and satellites are expected to be affected differently. This seems contrary to the results that the quenching efficiencies of centrals and satellites are correlated with halo mass and galaxy mass in a similar way. Our results thus suggest that ram pressure stripping alone cannot be the dominant quenching processes for the whole population. Similar argument may also be made for tidal stripping. However, since the effect of the tidal stripping is determined by the local mass density relative to the mass density of the galaxy to be stripped, this effect may also be important in relatively low-mass halos,

which may be in better agreement with observation.

The dependence of quenching on halo-centric radius for low-mass galaxies suggests that the significance of the underlying physical processes depends on the locations of galaxies in their host halos. The satellite-specific processes, such as ram pressure stripping and tidal stripping, are expected to be more efficient near the halo center, and so may be able to produce the dependence on halo-centric radius observed in the data. However, as discussed above, if these processes dominate the quenching of satellites and do not operate on centrals, then why do central galaxies have quenching properties similar to satellite galaxies of the same stellar masses? It may be that centrals are not special, and these satellite-specific processes also operate on centrals. This is in fact consistent with the fact that centrals are not at rest within the halo potential wells, and not even located at the halo center (e.g. Skibba et al. 2011). Indeed, one of the main conclusions that can be drawn from our results is that the central in a halo is not special, as far as its star formation quenching is concerned. Peng et al. (2010) found that the environmental quenching and mass quenching can be well separated from each other for galaxies at  $z \sim 1$ . It suggests that such a conclusion also holds for these galaxies. However, as mentioned above, this similarity between centrals and satellites is not expected in some galaxy formation models, where centrals and satellites are assumed to be affected by different quenching processes.

The processes discussed above, which are all confined within halos, can not account for the residual dependence on environmental density after removing the halo-mass effects. We thus include halo assembly history as an additional parameter, which is known to be influenced by large scale environment (e.g. Gao et al. 2005). Local tidal field is thought to play a key role in shaping the halo assembly bias (Wang et al. 2007; 2011a; Hahn et al. 2009; Shi et al. 2015; Paranjape et al. 2017; Borzyszkowski et al. 2017). For example, for a small halo in a high density region, the material around the halo is accelerated by the local tidal field so that the halo growth is significantly suppressed. These processes (on the scale much larger than the galactic scale) are unlikely to directly influence the star formation in galaxies.

Therefore, a correlation between the star formation and the halo assembly history has to be introduced in order to explain the residual dependence. It is worthwhile to note that it is unclear whether these large scale processes affect baryonic gas and dark matter in the same way. If it is not, additional effect on star formation should be taken into account.

The discussions given above provide some qualitative assessments about some of the quenching processes that have proposed in the literature, in connection to the observational results we find in this paper. To constrain theoretical models in a quantitative way, however, detailed modeling of the various quenching processes, as well as thorough analyses of all potentially important observational selection effects are needed. In a forthcoming paper, we will use mock catalogs constructed from hydrodynamic simulations and semi-analytic models of galaxy formation to compare galaxy formation models with the observational results obtained here (E. Wang et al. in preparation).

#### ACKNOWLEDGMENTS

We thank an anonymous referee for a useful report. This work is supported by the 973 Program (2015CB857002), NSFC (11522324, 11733004, 11421303, 11233005, 11621303), and the Fundamental Research Funds for the Central Universities. H.J.M. would like to acknowledge the support of NSF AST-1517528 and NSFC-11673015. S.H.C and Y.Y. are supported by the Fund for Fostering Talents in Basic Science of the National Natural Science Foundation of China NO.J1310021. FvdB is supported by the Klaus Tschira Foundation and by the US National Science Foundation through grant AST 1516962. WC is supported by the *Ministerio de Economía y Competitividad* and the *Fondo Europeo de Desarrollo Regional* (MINECO/FEDER, UE) in Spain through grant AYA2015-63810-P as well as the Consolider-Ingenio 2010 Programme of the *Spanish Ministerio de Ciencia e Innovación* (MICINN) under grant MultiDark CSD2009-00064. The work is also supported by the Supercomputer Center of University of Science and Technology of China and the High Performance Computing Resource in the Core Facility for Advanced Research Computing at Shanghai Astronomical Observatory.

#### REFERENCES

- Abazajian K. N., et al., 2009, *ApJS*, 182, 543-558  
 Baldry I. K., Glazebrook K., Brinkmann J., Ivezić Ž., Lupton R. H., Nichol R. C., Szalay A. S., 2004, *ApJ*, 600, 681  
 Baldry I. K., Balogh M. L., Bower R. G., Glazebrook K., Nichol R. C., Bamford S. P., Budavari T., 2006, *MNRAS*, 373, 469  
 Behroozi P. S., Conroy C., Wechsler R. H., 2010, *ApJ*, 717, 379  
 Bell E. F., McIntosh D. H., Katz N., Weinberg M. D., 2003, *ApJS*, 149, 289  
 Berti A. M., Coil A. L., Behroozi, P. S., Eisenstein D. J., Bray A. D., Cool R. J., Moustakas J., 2017, *ApJ*, 834, 87  
 Best P. N., von der Linden A., Kauffmann G., Heckman T. M., Kaiser C. R., 2007, *MNRAS*, 379, 894  
 Blanton M. R., et al., 2005, *AJ*, 129, 2562  
 Blanton M. R., Roweis S., 2007, *AJ*, 133, 734  
 Bluck A. F. L., Mendel J. T., Ellison S. L., Moreno J., Simard L., Patton D. R., Starkenburg E., 2014, *MNRAS*, 441, 599  
 Bluck A. F. L., et al., 2016, *MNRAS*, 462, 2559  
 Borzyszkowski M., Porciani C., Romano-Diaz E., Garaldi E., 2017, *MNRAS*, 469, 594  
 Bower R. G., Benson A. J., Malbon R., Helly J. C., Frenk C. S., Baugh C. M., Cole S., Lacey C. G., 2006, *MNRAS*, 370, 645  
 Brinchmann J., Charlot S., White S. D. M., Tremonti C., Kauffmann G., Heckman T., Brinkmann J., 2004, *MNRAS*, 351, 1151  
 Cacciato M., van den Bosch F. C., More S., Mo H., Yang X., 2013, *MNRAS*, 430, 767  
 Cui W., Borgani S., Murante G., 2014, *MNRAS*, 441, 1769  
 Cooray A., 2006, *MNRAS*, 365, 842  
 Croton D. J., et al., 2006, *MNRAS*, 365, 11  
 Dekel A., Birnboim Y., 2006, *MNRAS*, 368, 2  
 Dressler A., 1980, *ApJ*, 236, 351  
 Fabian A. C., 2012, *ARA&A*, 50, 455  
 Font A. S., et al., 2008, *MNRAS*, 389, 1619  
 Fossati M., et al., 2017, *ApJ*, 835, 153  
 Gao L., Springel V., White S. D. M., 2005, *MNRAS*, 363, L66  
 Gabor J. M., Davé R., Finlator K., Oppenheimer B. D., 2010, *MNRAS*, 407, 749  
 Guo Q., et al., 2011, *MNRAS*, 413, 101  
 Haas M. R., Schaye J., Jeon-Daniel A., 2012, *MNRAS*, 419, 2133  
 Hahn O., Porciani C., Dekel A., Carollo C. M., 2009, *MNRAS*, 398, 1742  
 Hearin A. P., Watson D. F., 2013, *MNRAS*, 435, 1313

- Hearin A. P., Watson D. F., van den Bosch F. C., 2015, *MNRAS*, 452, 1958
- Henriques B. M. B., White S. D. M., Thomas P. A., Angulo R., Guo Q., Lemson G., Springel V., Overzier R., 2015, *MNRAS*, 451, 2663
- Henriques B. M. B., White S. D. M., Thomas P. A., Angulo R. E., Guo Q., Lemson G., Wang W., 2016, arXiv, arXiv:1611.02286
- Hirschmann M., De Lucia G., Wilman D., Weinmann S., Iovino A., Cucciati O., Zibetti S., Villalobos Á., 2014, *MNRAS*, 444, 2938
- Hogg D. W., et al., 2003, *ApJ*, 585, L5
- Jing Y. P., Mo H. J., Börner G., 1998, *ApJ*, 494, 1
- Jing Y. P., Suto Y., Mo H. J., 2007, *ApJ*, 657, 664
- Kang X., Jing Y. P., Mo H. J., Börner G., 2005, *ApJ*, 631, 21
- Kang X., van den Bosch F. C., 2008, *ApJ*, 676, L101
- Kauffmann G., White S. D. M., Heckman T. M., Ménard B., Brinchmann J., Charlot S., Tremonti C., Brinkmann J., 2004, *MNRAS*, 353, 713
- Kauffmann G., Li C., Zhang W., Weinmann S., 2013, *MNRAS*, 430, 1447
- Kereš D., Katz N., Weinberg D. H., Davé R., 2005, *MNRAS*, 363, 2
- Knobel C., et al., 2013, *ApJ*, 769, 24
- Knobel C., Lilly S. J., Woo J., Kovač K., 2015, *ApJ*, 800, 24
- Kravtsov A. V., Berlind A. A., Wechsler R. H., Klypin A. A., Gottlöber S., Allgood B., Primack J. R., 2004, *ApJ*, 609, 35
- Kroupa P., 2001, *MNRAS*, 322, 231
- Lacerna I., Padilla N., Stasyszyn F., 2014, *MNRAS*, 443, 3107
- Lange J. U., van den Bosch F. C., Hearin A., Campbell D., Zentner A. R., Villarreal A., Mao Y.-Y., 2017, preprint (arXiv:1705.05043)
- Leclercq F., Lavaux G., Jasche J., Wandelt B., 2016, *JCAP*, 8, 027
- Li Y., Mo H. J., Gao L., 2008, *MNRAS*, 389, 1419
- Liu L., Yang X., Mo H. J., van den Bosch F. C., Springel V., 2010, *ApJ*, 712, 734
- Lim S. H., Mo H. J., Wang H., Yang X., 2016, *MNRAS*, 455, 499
- Lim S. H., Mo H. J., Lan T.-W., Ménard B., 2017, *MNRAS*, 464, 3256
- Lu Y., Mo H. J., Weinberg M. D., Katz N., 2011, *MNRAS*, 416, 1949
- Lu Z., Mo H. J., Lu Y., Katz N., Weinberg M. D., van den Bosch F. C., Yang X., 2014, *MNRAS*, 439, 1294
- Lu Z., Mo H. J., Lu Y., Katz N., Weinberg M. D., van den Bosch F. C., Yang X., 2015, *MNRAS*, 450, 1604
- Mandelbaum R., Seljak U., Kauffmann G., Hirata C. M., Brinkmann J., 2006, *MNRAS*, 368, 715
- Mo H. J., Mao S., White S. D. M., 1999, *MNRAS*, 304, 175
- Mo H., van den Bosch F. C., White S., 2010, *Galaxy Formation and Evolution* (Cambridge: Cambridge University Press).
- Mo H. J., White S. D. M., 1996, *MNRAS*, 282, 347
- Mo H. J., Yang X., van den Bosch F. C., Katz N., 2005, *MNRAS*, 363, 1155
- Moster B. P., Naab T., White S. D. M., preprint (arXiv:1705.05373)
- Navarro J. F., Frenk C. S., White S. D. M., 1997, *ApJ*, 490, 493
- Neistein E., van den Bosch F. C., Dekel A., 2006, *MNRAS*, 372, 933
- Ocvirk P., Pichon C., Teyssier R., 2008, *MNRAS*, 390, 1326
- Oemler A., Jr., 1974, *ApJ*, 194, 1
- Paranjape A., Hahn O., Sheth R. K., 2017, arXiv, arXiv:1706.09906
- Pasquali A., Gallazzi A., Fontanot F., van den Bosch F. C., De Lucia G., Mo H. J., Yang X., 2010, *MNRAS*, 407, 937
- Peacock J. A., Smith R. E., 2000, *MNRAS*, 318, 1144
- Peng Y.-j., et al., 2010, *ApJ*, 721, 193
- Peng Y.-j., Lilly S. J., Renzini A., Carollo M., 2012, *ApJ*, 757, 4
- Schaye J., et al., 2015, *MNRAS*, 446, 521
- Skibba R. A., 2009, *MNRAS*, 392, 1467
- Skibba R. A., van den Bosch F. C., Yang X., More S., Mo H., Fontanot F., 2011, *MNRAS*, 410, 417
- Sheth R. K., Mo H. J., Tormen G., 2001, *MNRAS*, 323, 1
- Shi F., et al., 2016, *ApJ*, 833, 241
- Shi J., Wang H., Mo H. J., 2015, *ApJ*, 807, 37
- Spindler A., Wake D., 2017, *MNRAS*, 468, 333
- Tinker J. L., Norberg P., Weinberg D. H., Warren M. S., 2007, *ApJ*, 659, 877
- Tinker J., Wetzel A., Conroy C., Mao Y.-Y., 2016, arXiv, arXiv:1609.03388
- Tweed D., Yang X., Wang H., Cui W., Zhang Y., Li S., Jing Y. P., Mo H. J., 2017, *ApJ*, 841, 55
- Vale A., Ostriker J. P., 2006, *MNRAS*, 371, 1173
- van den Bosch F. C., Aquino D., Yang X., Mo H. J., Pasquali A., McIntosh D. H., Weinmann S. M., Kang X., 2008, *MNRAS*, 387, 79
- van den Bosch F. C., et al., 2007, *MNRAS*, 376, 841
- Vogelsberger M., et al., 2014, *MNRAS*, 444, 1518
- Wang H. Y., Mo H. J., Jing Y. P., 2007, *MNRAS*, 375, 633
- Wang H., Mo H. J., Jing Y. P., Yang X., Wang Y., 2011, *MNRAS*, 413, 1973
- Wang H., Mo H. J., Yang X., van den Bosch F. C., 2012, *MNRAS*, 420, 1809
- Wang H., Mo H. J., Yang X., Jing Y. P., Lin W. P., 2014, *ApJ*, 794, 94
- Wang H., et al., 2016, *ApJ*, 831, 164
- Wang H., Wang T., Zhou H., Liu B., Wang J., Yuan W., Dong X., 2011b, *ApJ*, 738, 85
- Wechsler R. H., Zentner A. R., Bullock J. S., Kravtsov A. V., Allgood B., 2006, *ApJ*, 652, 71
- Weinmann S. M., Kauffmann G., van den Bosch F. C., Pasquali A., McIntosh D. H., Mo H., Yang X., Guo Y., 2009, *MNRAS*, 394, 1213
- Weinmann S. M., Kauffmann G., von der Linden A., De Lucia G., 2010, *MNRAS*, 406, 2249
- Weinmann S. M., van den Bosch F. C., Yang X., Mo H. J., 2006, *MNRAS*, 366, 2
- Wetzel A. R., Tinker J. L., Conroy C., 2012, *MNRAS*, 424, 232
- Wetzel A. R., Tinker J. L., Conroy C., van den Bosch F. C., 2013, *MNRAS*, 432, 336
- White S. D. M., Frenk C. S., 1991, *ApJ*, 379, 52
- White S. D. M., Rees M. J., 1978, *MNRAS*, 183, 341
- Woo J., et al., 2013, *MNRAS*, 428, 3306
- Woo J., Dekel A., Faber S. M., Koo D. C., 2015, *MNRAS*, 448, 237
- Yang X., Mo H. J., van den Bosch F. C., 2003, *MNRAS*, 339, 1057
- Yang X., Mo H. J., van den Bosch F. C., Jing Y. P., 2005, *MNRAS*, 356, 1293
- Yang X., Mo H. J., van den Bosch F. C., 2006, *ApJ*, 638, L55
- Yang X., Mo H. J., van den Bosch F. C., Pasquali A., Li C., Barden M., 2007, *ApJ*, 671, 153
- Yang X., Mo H. J., van den Bosch F. C., 2009, *ApJ*, 695, 900
- Yang X., Mo H. J., van den Bosch F. C., Zhang Y., Han J., 2012, *ApJ*, 752, 41
- Yang X., Mo H. J., van den Bosch F. C., Bonaca A., Li S., Lu Y., Lu Y., Lu Z., 2013, *ApJ*, 770, 115
- York D. G., et al., 2000, *AJ*, 120, 1579
- Zheng Z., et al., 2005, *ApJ*, 633, 791
- Zheng Z., et al., 2017, *MNRAS*, 465, 4572
- Zu Y., Mandelbaum R., 2016, *MNRAS*, 457, 4360